

Anonymous Referee #1

Received and published: 29 December 2018

Review of Pearson et al.

This manuscript provides a detailed analysis of long term atmospheric chemical measurements at sites in Alaska. The authors provide a wealth of statistical and back trajectory analyses and the wealth of information is well presented. This manuscript will be of interest to a variety of readers and is well suited for ACPD. There are a lot of small grammatical and typographical errors and it is frustrating to see this and have to address it all. In the future I recommend all authors read and edit and fix these issues as I do not feel it is a Reviewer's job to fix grammar and punctuation. That said I recommend minor editing and a few suggestions but overall I strongly recommend this for publication.

General comments keyed to the text:

12: no comma after Service

Removed comma.

13: after "years." I recommend a sentence identifying the locations of the stations. I also recommend mentioning here that there are data from a variety of other metals otherwise at line 31 we see mention of the other metals.

We believe we already appropriately give the location of the five stations in the abstract, and highlight in line 14 that additional metals (Cr, Ni, As, and Pb) were analysed.

16: were statistically significantly?

Modified wording to "statistically higher"

30: here and elsewhere (line 38) it is "in between" with no hyphen

Edited to consistently use "in-between" throughout paper.

66: to Alaska

Corrected.

76: study of

Corrected.

78: Perhaps a sentence here providing context for Hg deposition attribution from other locations?

Perhaps the Lower 48 since that is brought in later for the other metals. Is 57% high, low, or likely about average for global sources and deposition?

Added citation for context:

This estimate may be high given that globally, anthropogenic Hg emissions are estimated to account for approximately 30% of total atmospheric sources (i.e., total anthropogenic and natural emissions plus re-emission) (UNEP 2013).

86: Program's

Corrected.

98-101: I like that a little description of the terrain and vegetation is given for the Gates of the Arctic site but what about the others? Add some more info please. Maybe a sentence for each site?

Added additional vegetation and landcover descriptions for each site.

128-9: “due to the low sample volume collected for each deposition sample”?
Edited to “due to low sample volumes collected during sampling”

220: The highest
Corrected.

231: also occur
Corrected.

232: and decrease
Corrected.

249: Gates
Corrected.

259-264: what about the typical and long term different fractions of wet and dry precipitation at each site? Is this changing over time? How were snow samples collected? And is there any sense that the dry precipitation is shifting towards wet? Particularly at the more northern sites? This could feed into some comments I have later about the future deposition. Were there any major storm events that stood out in the analysis? I realize long precip event samples were broken up but can they be pieced back together to identify how/where large precip events may affect the overall yearly deposition at a site? I realize this may be a giant analysis that I do not want to send the authors out on but I am curious. This is sort of addressed in the next few lines.

We clarify that all samples were collected using the standard NADP wet deposition sampling protocols which do not analyze individual storms based on 2-week sampling periods in the NADP program. However, we already discuss the close relationships between deposition concentrations/amounts and precipitation size in detail in section 3.1. (We determined that the major reason for higher Hg concentrations at northern sites was a lower dilution (or “wash-out” effect) of Hg concentrations by smaller storm sizes (Figure 1 and discussion below)...and following paragraph.)

The reviewer is correct about the importance of dry deposition. We added a short section in paragraph 3.2.1. about the importance of dry deposition that is based on recent studies in the Arctic tundra.

280: the MDN
Corrected.

328-9: This is an extremely important finding. Figure 4a: why do Gates of the Arctic and Nome have seemingly anomalously higher values (ie the small circles of higher color keyed values) only where the stations are located? I assume some sort of kriging of data analysis artefact?

The “hotspots” of seemingly higher values at Gates of the Arctic and Nome are due to limitations with IDW interpolation and a small number of sites. We applied IDW to follow standard methods developed by NADP utilized for CONUS deposition mapping. In general, the concentration map agrees with the precipitation map and shows higher concentration in the dryer northern portions of AK and lower concentrations at the wetter southern and coastal sites. We caution readers about the limitations of applying spatial interpolation with such a limited number of sites, but felt that the overall figure demonstrates the spatial patterns found between these five sites.

394: Since Denali National Park is mentioned. Isn't there some data or results from Denali? Again I do not want the authors to spend a lot of time on this but I wonder if there are similar results or analyses from any other locations. Or other studies with similar approach applied to Alaska that could be referenced? What about the long term DOE air monitoring sites- do they measure metals or Hg?

To our knowledge, there are no published wet deposition studies of Hg in Alaska, with the exception of the study by Jaeglé we cite in the manuscript.

395: amounts

Corrected.

401: maps of estimated

Corrected.

418: remove "deposition" after "lowest"

Corrected.

419-420: "individual used twice. Can this be cleaned up to one mention of "individual"?"

Corrected.

435-445: This is an interesting result of the study.

523: elements

Corrected.

525: suggests. Here and elsewhere I recommend active and not passive tense.

Corrected here and throughout.

526: the results also support the possibility

Corrected.

530: crustal sources while (no comma)

Corrected.

533: in between and thereby do not indicate (if you agree to shift to active tense)

Corrected.

General comment: There are an increasing number of studies showing that the Arctic is getting wetter, particularly that the winter is shortening and the snow to rain fraction is decreasing. Could the authors break their data into snow versus rain as the seasonal sources and then use potential projections to address who/where a wetter Arctic may affect deposition? At the least there should be some mention of how a warmer future Arctic and its' changing precipitation dynamic may affect loadings.

We added a few sentences in the summary section discussing impact of global warming and arctic amplification on Hg deposition and other relevant ecosystem processes. While we cannot discuss specific responses on Hg deposition, we highlight global warming will result in complex, yet poorly understood, consequences of climate change on Arctic Hg exposure.

Figure 2: how were the different season parsed? And were snow versus rain events separated? I realize the coastal sites may see lots of winter rain but I am curious again at the snow versus rain breakdowns.

We added season definitions to Figure text for clarity.

Figure 5: The areas projected by the true color images (ie the map area) are slightly different. I recommend providing one consistent background and maps at the same scale to show the different source regions and distances of back trajectories.

Figure was regenerated to use same spatial extent for all plots.

Interactive comment on “Mercury and trace metal wet deposition across five stations in Alaska: controlling factors, spatial patterns, and source regions” by Christopher Pearson et al.

Anonymous Referee #2

Received and published: 2 January 2019

Here are a few concerns this reviewer has. One problem is their analysis of “precipitation origins/sources”. Precipitation formation is in large part driven by microphysics; it is not like pollutants that can be transported from upwind source regions. This sort of analysis and language is really odd. Hence quite a bit of their “intensive” trajectory analysis for “precipitation origins/sources” is not valid.

This is a good point. We removed the trajectory analyses for precipitation origins/sources, and now only present the analysis for Hg deposition. We also adjusted the text accordingly.

Section 2.2 is not necessary.

We disagree (see also comments below). While we agree that there are in fact only five stations, we strongly feel that providing these maps ideally highlights that large parts of this northern parts is expected to have very low Hg deposition loads due to low precipitation amounts. We provided sufficient caution to read these maps in the text and highlight the limitations of the maps as well.

The maps were extrapolated from 5 sites only apparently with too large uncertainties. For instance, the spatial distributions of Hg concentrations can be quite complex. Their results showed that Dutch Harbor saw a similar precipitation amount to that at Glacier but had a median Hg concentration >50% greater, and Kodiak had >30% more precipitation and >15% more Hg concentration than those at Glacier. How to reconcile these disparate spatial differences? Why would one expect simplistic linear extrapolation to capture these differences?

Our inverse-distance weighted interpolation maps follow procedures developed by the National Atmospheric Deposition Program, which creates CONUS wide maps of annual Hg deposition. Following a similar methodology allows readers to directly compare maps from this analysis to maps produced by NADP. The concentration and deposition maps highlight larger-scale spatial patterns (i.e. North/South, East/West) and will not (and are not intended to) fully capture or model smaller scale deposition trends related to geographic and point/local sourcing. Throughout this section, we clearly mention the limitations of this analysis. As our analysis shows, precipitation is the largest control on annual deposition, and hence the use of the Reanalysis Precipitation product is a valid approach to capture the overall spatial patterns of Hg deposition across this region. We strongly feel that this mapping is very useful to pinpoint the areas of particular concern for Hg deposition and further expansion and investment of monitoring networks.

Section 3.3 needs to be redone. First the authors conducted a PCA analysis. Usually one uses tracers that represent distinctly different sources, but the metals they used could not seem to do the job. It was not clear why they did a PCA of the metals to begin with. Since Al measurements were not available, the authors decided that Cr and Ni can be used as alternatives of Al, a crustal tracer. Where did they get [xucc]/[Cruc] or [xucc]/[Niucc]? At one point the authors decided that Asian pollution could influence Alaska based on As and Pb (line 489). But there are major anthropogenic sources for Cr and Ni in Asia as well. It was unclear what the authors were trying to do with Figure 6. No interpretation was given but merely description of how the first two components were positively or negatively correlated. What do those correlations really mean?

We clarified the PCA section. Specifically we identified PC1 as Precipitation with all elements showing a negative correlation due to washout effects. Hg's relationship to PC1 (precipitation) was slightly different from the other metals due to its reactive nature and susceptibility to gaseous reemission.

This manuscript can be shortened significantly, by removing tutorial material, redundancy, repetition, and passages that merely pointed out the obvious. To be specific, Section 2 can be cut down quite a bit by removing the tutorial stuff in the statistics and trajectory sections.

We significantly shortened Section 2.2; however, key elements related to the data treatment and statistical handling were left as we feel it is important to highlight data processing (such as treatment of outliers and below detection limit values). Section 2.3 was also shortened to include only key information related to the HYSPLIT model and data processing. Finally, we removed the discussion of backtrajectory analysis for precipitation as well as suggested above.

In their results and discussion sections they often stated the obvious.

We edited the manuscript and tried to remove non-critical text and "obvious" discussion related to the interpretation of our results.

List of Relevant Changes

- General grammar and punctuation edits occurred throughout manuscript
- Site descriptions were expanded for clarity
- Redundant background information on statistical tests was removed throughout
- Wordy and obvious discussion of results was removed throughout
- The Enrichment Factor Analysis was found to be flawed and was removed
- Back trajectory analysis related to precipitation origins was removed
- Additional discussion of the PCA was added to better frame the observed correlations
- Additional discussion and citations related to impacts of warming and snow/rain transitions was added to the conclusions section
- Figure 5: We removed the precipitation weighted maps and edited the other back trajectory figures to show a consistent extent
- Additional p-values were added to Table 2 for clarity

Mercury and trace metal wet deposition across five stations in Alaska: controlling factors, spatial patterns, and source regions

Christopher Pearson¹, Dean Howard², Christopher Moore^{3,4}, and Daniel Obrist^{2,3}

¹Division of Hydrologic Sciences, Desert Research Institute, Reno, NV, USA

²Department of Environmental, Earth, and Atmospheric Sciences, University of Massachusetts-Lowell, Lowell, MA, USA

³Division of Atmospheric Sciences, Desert Research Institute, Reno, NV, USA

⁴Gas Technology Institute, Des Plaines, IL, USA

Correspondence to: Daniel_Obrist@uml.edu

Abstract. A total of 1,360 weeks of mercury (Hg) wet deposition data were collected by the State of Alaska Department of Environmental Conservation and the U.S. National Park Service: across five stations ~~covering~~ spanning up to eight years. Here, we analyse concentration patterns, source regions, and seasonal and annual Hg deposition loadings across these five sites in Alaska, along with auxiliary trace metals including Cr, Ni, As, and Pb.

We found that Hg concentrations in precipitation at the two northern-most stations, Nome (64.5° N) along the coast of the Bering Sea and the inland site of Gates of the Arctic (66.9° N), were significantly-statistically higher (average of 5.3 ng L⁻¹ and 5.5 ng L⁻¹, respectively) than those at the two lowest-latitude sites, Kodiak Island (57.7° N, 2.7 ng L⁻¹) and Glacier Bay (58.5° N, 2.6 ng L⁻¹). These differences were largely explained by different precipitation regimes, with higher ~~amounts of~~ precipitation at the lower latitude stations leading to dilution effects. Highest annual Hg deposition loads were consistently observed at Kodiak Island (4.80 +/- 1.04 µg m⁻²), while lowest annual deposition was at Gates of the Arctic (2.11 +/- 0.67 µg m⁻²). Across all stations and collection years, annual precipitation overwhelmingly-strongly controlled annual Hg deposition, explaining 73% of the variability in observed annual Hg deposition. ~~Our~~ The data analyses further showed that annual Hg deposition loads across all five Alaska sites were consistently among the lowest in the United States, ranking in the lowest 1 to 5 percent of over 99 monitoring stations.

Detailed back trajectory analyses showed diffuse source regions for most Hg deposition sites, ~~which were almost identical with precipitation origins~~, suggesting largely global or regional Hg sources. One notable exception was Nome where we found pronounced differences between precipitation and Hg source origins with increased Hg contributions from the western Pacific Ocean downwind of East Asia. Analysis of ~~multiple other~~ trace elements (As, Cr, Cu, Ni, Pb, Se, Zn) from Dutch Harbor, Nome, and Kodiak Island showed generally higher trace metal concentrations at the

northern station Nome compared to Kodiak Island further to the south, with concentrations at Dutch Harbor falling in-between. Across all sites, we find two distinct groups of correlating elements: Cr and Ni and As and Pb. We attribute these associations to possibly different source origins, whereby sources of Ni and Cr may be derived from crustal (e.g., dust) sources while As and Pb may include long-range transport of anthropogenic pollution, ~~and~~ Neither Hg nor any of the other trace elements analyzed, consistently associated with these was not associated strongly with either of these two groups of elements, suggesting largely diffuse source origins. Calculations of enrichment factors (i.e., elemental enrichment compared to the upper continental crust) show low enrichment for Cr and Ni which is in support

Commented [OD1]: Specify which ones.

of a predominantly crustal source. High enrichment factors for Pb and Se are indicative of anthropogenic or additional natural sources for these elements. For most other elements including Hg, enrichment factors fell in between these groups showing no clear source attribution to either crustal or anthropogenic source origins.

40

1. Introduction

The land surface area of the State of Alaska is approximately one-fifth of that of the contiguous United States, but little spatial information is available on pollutant deposition and impacts affecting local ecosystems, wildlife, and humans. Most contaminant studies have focused on the Arctic domain, including studies conducted by large international collaborative efforts such as the Arctic Monitoring and Assessment Program (AMAP), a working group of the Arctic Council (AMAP, 2009a, b, 2011). The interests in northern latitude pollutant studies are driven by reports that show significant neurotoxicity as well as immunological, cardiovascular, and reproductive effects in Arctic populations and wildlife from exposure to contaminants (AMAP, 2011). Important pollutants found in northern arctic and boreal areas include mercury (Hg) – which is the focus of the current analysis – as well as persistent organic pollutant (POPs), polycyclic aromatic hydrocarbons (PAHs) and other trace metals such as lead (Pb) and cadmium (Cd) that are primarily supplied to the region by atmospheric transport and deposition (AMAP, 2005, 2009b, 2011). The major concerns of these pollutants are their toxicity and persistency in the environment. Delivery of contaminants to the high Arctic is expected to increase in the future due to changes in synoptic atmospheric transport patterns and an expected increase in contaminant source fluxes related to increased development, resource extraction, and transportation activities within northern regions (Jaeglé, 2010; Streets et al., 2011).

Mercury is a neurotoxic pollutant significantly affecting northern latitudes, with human exposure mainly derived from consumption of seafood and marine mammals that are part of traditional diets based on hunting and fishing (Stow et al., 2011). Risks associated with long-term exposures to Hg, particularly to the organic monomethyl-Hg (MeHg), include neuro-developmental delays in children exposed in utero, impaired cardiovascular health in adults, and disruption of immunological and endocrine functions (Karagas et al., 2012; Tan et al., 2009). Hg biomagnifies in aquatic and terrestrial food webs and is present at elevated concentrations in northern wildlife such as seals, polar bears, beluga whales, Arctic foxes, birds, and fish (Lawson and Mason, 1998; Watras and Bloom, 1992; Baeyens et al., 2003; Loseto et al., 2008; Evans et al., 2005; Dietz et al., 2009; Walker et al., 2006; Outridge et al., 2008; Douglas et al., 2012; Macdonald and Bewers, 1996; Leitch et al., 2007; Braune et al., 2014; Bocharova et al., 2013; Laird et al., 2013; Ackerman et al., 2016; Eagles-Smith et al., 2016). Long-range transport via the atmosphere is considered the primary source of Hg deposition to Alaska the high latitudes (Dommergue et al., 2010; Steffen et al., 2008). In addition, springtime photochemical reactions, termed Atmospheric Mercury Depletion Events (AMDEs), lead to additional Hg deposition to snow and ice, particularly along the Arctic Ocean coast (Douglas and Sturm, 2004; Lindberg et al., 2002). Regional and local sources of atmospheric Hg exist in Alaska both from natural and anthropogenic emissions. The EPA Toxics Release Inventory (TRI) reported total air emissions of Hg and Hg compounds in Alaska of 24 kg (53 lbs) from both fugitive and point-source air sources in 2014 (Table 1; EPA, 2014). Other sources include natural emissions from wildfires (Mitchell et al., 2012; Wiedinmyer et al., 2006; Turetsky et al., 2006; Friedli et al., 2001; Brunke et al., 2001; Webster et al., 2016; Obrist et al., 2008), volcanic emissions (Mather and Pyle, 2004; Pyle

and Mather, 2003;Nriagu and Becker, 2003;Ferrara et al., 2000), and degassing from Hg-enriched soils and possibly background soils (Agnan et al., 2015a;Gustin et al., 2008), although many of these sources are poorly constrained across Alaska. Jaeglé (2010) conducted a detailed study on atmospheric sources of Hg contamination over Alaska using GEOS-Chem model simulations and suggested that anthropogenic emissions contribute approximately 57% of Hg deposition over Alaska, with other sources dominated by natural land (i.e. volcanos, wild fires) and ocean-based emissions. The estimated anthropogenic contributions seem quite given that Globally, anthropogenic Hg emissions are estimated to account for approximately 30% of total atmospheric sources (i.e., total anthropogenic and natural emissions plus re-emission) (UNEP 2013). Lindberg, et al. estimated that anthropogenic sources account for approximately 36% of emissions, while natural land and ocean sources account for 24% and 39%, respectively.

Here we analyse Alaska Hg wet deposition data collected by the State of Alaska and the National Park Service between 2007 and 2015 across five Hg wet deposition stations in Alaska. Deposition sites are Gates of the Arctic, Nome, Glacier Bay National Park, Kodiak, and Dutch Harbor (Table 1; Figure 4). Please refer to Figure 4 for a map of site locations. The dataset contains 1360 weeks of total measurements across the five stations, with the longest record lasting almost 8 years, allowing for analysis of temporal, seasonal, and spatial patterns of Hg wet deposition across Alaska. All measurements were conducted according to trace metal sampling protocols following the National Atmospheric Deposition Program's (NADP) Mercury Deposition Network (MDN) standards. We use statistical tests to compare deposition concentrations, loads, and seasonal and inter-annual patterns to assess variables controlling Hg deposition. In addition, we performed detailed back trajectory analyses for full annual datasets at select stations to quantify source regions that contribute to annual Hg deposition loads. We further use deposition data of auxiliary trace metals, including Cr, Ni, As, and Pb, to identify associations with Hg and among these trace elements and to derive enrichment factors and source patterns. Finally, we performed spatial scaling and mapping of annual wet deposition of Hg throughout all of Alaska based on observed concentration gradients and precipitation distributions.

2. Materials and Methods

2.1. Collection and analysis of Hg Deposition data and ten additional trace elements

Weekly Hg deposition data were collected from five wet deposition stations in Alaska operated by the State of Alaska Division of Environmental Conservation and the National Park Service. Deposition stations include Gates of the Arctic, Nome, Glacier Bay National Park, Kodiak, and Dutch Harbor (Table 1; Please refer to Figure 4 for a map of site locations). Gates of the Arctic is a protected wilderness area in northern Alaska consisting of multiple mountain ranges and sparse boreal forests. Nome is at sea level located on the western coast of Alaska off the Bering Sea. Nome's landscape is characterized as arctic tundra with ground brush vegetation and little tree cover. Glacier Bay National Park is a coastal site located in the northern section of the Alaska panhandle. Glacier Bay consists of wet tundra and dense coastal forest. Kodiak is a mountainous island located off the southern coast of Alaska. Low elevation vegetation consist of shrubs and grasses, while alpine tundra exists at higher elevations. Finally, Dutch Harbor is located on Amaknak Island in the Aleutian Islands. Most of the islands consists of dense shrubs with very little conifer growth. Sample collections were performed on a weekly basis using trace-metal wet-deposition collectors (Model MDN 00-125-4; N-Con Inc., Crawford, GA, USA), following MDN protocols for collection of Hg in precipitation (Mercury Deposition Network: Field Methods, 2017). In summary, the protocols include weekly collection using a

Commented [OD2]: UNEP (2013). Global Mercury Assessment 2013: Sources, Emissions, Releases and Environmental Transport. Geneva, Switzerland, United Nations Environment Programme.

Commented [CP3]: Add citation to references.

Formatted: Default Paragraph Font

Formatted: Highlight

specially modified NADP sampler. Each collection bottle and sample train was acid-cleaned prior to deployment and pre-charged with hydrochloric acid preservative. Analysis of samples for Hg were performed by Mercury Analytical Laboratory (HAL, Eurofins Frontier Global Sciences, Inc., Seattle, Washington, USA) according to EPA Methods 1669 and 1631.

115 ~~MDN~~Data coverage ~~varie~~eds by site and ranged from September 2007 to September 2015. The longest dataset is from Kodiak (2007 to 2015), followed by Gates of the Arctic (2008 to 2015), and Dutch Harbor (2009 to 2015). Both Glacier Bay (2010 to 2013) and Nome (2013 to 2015) had shorter datasets (less than 3 years). All sites ~~have-had~~ intermittent data gaps ranging from weeks to months. The most significant data gaps occurred at Kodiak during summers of 2009 and 2010, and Dutch Harbor during 2010, 2013, and 2014.

120 Detailed quality assurance and control of data followed the protocols of the NADP MDN. Each sample was assigned a quality rating (A, B, or C) based on collector performance, sample quality, and analytical measurement excellence. A ratings were assigned to samples of “highest quality” with no issues during collection or analysis, B ratings referred to data with minor problems, and C ratings referred to samples with significant defects. Samples with a rating of C were removed prior to our data analysis. During weeks with missing rain gage data, the measured volume of water
125 collected in the sample bottle was used as the precipitation measurement. Trace samples (unmeasurable by the rain gage) were assigned a precipitation value of 3.23 mm (following NADP MDN protocol).

In addition to the Hg deposition data, we analysed corresponding data of additional trace elements collected at three of the five Hg deposition stations: Dutch Harbor, Kodiak Island, and Nome. Available analysis of trace elements includes the following 10 additional elements: arsenic (As), beryllium (Be, cadmium (Cd), chromium (Cr), copper
130 (Cu), lead (Pb), nickel (Ni), ~~se~~Selenium (Se), and zinc (Zn). Trace metal analysis was performed by inductively coupled plasma mass spectrometry following EPA Method 200.8 (Brockhoff et al., 1999). Seven of these trace elements are listed on EPA’s list of hazardous air pollutants (EPA, 2016), including As, Be, Cd, Cr, Pb, Ni, and Se. In total, there were 132 trace element deposition samples. Dutch Harbor had a total of 24 samples collected from 9/24/20113 through 4/28/2015, Nome had a total of 42 samples between 10/30/2013 and 4/28/2015, and Kodiak Island
135 had a total of 65 samples between 9/17/2013 and 4/28/2015. We assumed that large gaps in data coverage were mainly due to low sample volumes collected during ~~deposition samplesampling~~, which often did not allow measurement of these trace metals. A significant number of samples showed trace element concentrations below the analytical detection limit. The percentage of samples below detection limits were as follows, from highest to lowest percentage: Cd: (80%), Be (56%), and Ni (44%), As (36%), and Cr (34%). All other elements had observations below reported
140 detection limits less than 6%. Be and Cd were not included in this current analysis due to their large percentage of missing values.

2.2. Statistical analyses, spatial interpolation, and mapping

All statistical analyses were performed using the statistical software program “R” (R-Core-Team, 2014). Specific R packages utilized throughout the analysis included ade4, ggplot, NADA, corrplot and psych (Lee, 2013; Dray and Dufour, 2007; Revelle, 2014; Wickham, 2009). Outliers for both the Trace Metal Dataset and NADP Hg Deposition dataset were determined using the 1.5 x Interquartile Range (IQR) rule. ~~Datasets were Log₁₀ transformed and back-transformed during outlier testing in order to account for the skewed right/log-normal distribution of the data.~~

~~Summary statistics are shown throughout this study using both the total data set and data sets with outliers removed.~~

The trace metal dataset contained several elements where significant portions of the data fell below detection limits (BDL). For these data, maximum likelihood estimation (MLE) summary statistics were calculated using the NADA package (Lee, 2013) in addition to 1/2 MDL substitution. In general, MLE and non-parametric techniques are preferred to be used for non-detect values since replacement of data (e.g., using 1/2 detection limits) can be problematic (Helsel, 2012). ~~In particular MLE has been shown to produce unbiased estimates of mean, median, and standard deviation without substitution for minimally censored data sets with n > 50 (Helsel, 2012).~~ A lognormal distribution was assumed for MLE estimation. ~~When applicable, non-parametric ranked based tests were performed on the trace metal dataset. Boxplots and scatterplots were made using the ggplot2 package (Wickham, 2009).~~

~~Analysis of Variance (ANOVA) and Analysis of Covariance (ANCOVA) were performed using the aov function in the R stats package (R Core Team, 2014).~~ Analysis of Variance (ANOVA) and Analysis of Covariance (ANCOVA) ~~were~~ Testing was performed on Log10-transformed data using a type-III ANOVA to account for unbalanced factor levels in the dataset. Trace metal ANOVAs were performed on the 1/2 MDL substituted datasets.

~~Trace metal correlations were assessed by the non-parametric Kendall Tau test to account for BDL substitution and tied rankings. Kendall's test does not require any assumptions about the underlying distribution of the dataset and is less sensitive to tied values in the ranking process. Correlation testing was performed using the psych package (Revelle, 2014) and visualized with the corplot package.~~

~~A principal component analysis (PCA) using the R package ade4 (Dray and Dufour, 2007) was performed on the ranked trace metal dataset. The A trace metal PCA for all trace metals was performed on ranked data to account for BDL values and non-normal distributions. Season was defined as follows for both datasets: Spring (March, April, May), Summer (June, July, August), Fall (September, October, November), Winter (December, January, February).~~

Mapping and spatial interpolation and extrapolation of Hg deposition loads were performed in ArcGIS®. Inverse distance weighting (n=5; p=0.5) was used to interpolate and extrapolate precipitation weighted mean concentrations (PWM) across Alaska. ~~The processing extent was allowed to extend beyond the sampling region to cover the entire State of Alaska.~~ Precipitation weighted mean Hg concentrations were used from NADP MDN annual estimates and averaged for all available years. MDN annual estimates were only available for years with i) Hg sampling covering ≥75% of the sampling period ii) Hg measurements of >75% of annual precipitation events and iii) >90% coverage of total annual precipitation (either gage or sample bottle). The estimated PWM Hg concentrations were then combined with annual normal precipitation averaged for the period of 2007-2015 from the NCEP Climate Forecast System Version 2 (CFSv2) 6-hourly Products (Saha, 2011) to estimate deposition totals across the State of Alaska. Precipitation data was accessed and compiled using Google Earth Engine (Google Earth Engine Team, 2015).

2.3. Back-trajectory analysis and modeling and determination of deposition source areas

Backtrajectory ~~analyses utilized ies were generated using~~ the National Oceanic and Atmospheric Administration Air Resources Laboratory's Hybrid Single Particle Lagrangian Integrated Trajectory (HYSPLIT) Version 4 Model. ~~The model and associated files were accessed under: (http://ready.arl.noaa.gov/hyreg/HYSPLIT_pchysplit.php). Global Data Assimilation System (GDAS) 0.5 degree meteorological data The model was implemented with meteorological data from NOAA for use in the was used within the HYSPLIT model available (under:~~

Commented [OD4]: Please check

Formatted: Highlight

Formatted: Highlight

185 ~~<http://ready.arl.noaa.gov/archives.php>. Data used for this project was the Global Data Assimilation System (GDAS) 0.5 degree meteorological data.~~ We performed ~~an intensive analysis of the~~ backtrajectories analyses for each individual precipitation event for the entire year of 2014 for each station with available Hg wet deposition for that year (Nome, Gates of the Arctic and Kodiak Island). Individual precipitation events were considered when measurable precipitation data were present at the one-hour time resolution. If a storm lasted several hours without an interruption of storm activity, the event was classified as a single precipitation event; if there was an interruption in measurable precipitation >2hr in duration, the storm was separated into two events. Using this method, the number of precipitation events identified for 2014 were 247 (Kodiak Island), 182 (Nome), and 148 (Gates of the Arctic).

A single air parcel trajectory was calculated for each precipitation event, with the end time initialized to coincide with the center of each precipitation period along with the end latitude and longitude set to each monitoring station. The altitude at which all backtrajectories was initiated was set to 2,000 m a.s.l. ~~The output of each HYSPLIT run (trajectory) represents the latitude, longitude and altitude of an air parcel with these final coordinates over the previous 40 days, with temporal resolution of 1 hour (i.e. 240 3D coordinates per trajectory).~~

In order to delineate source regions for seasonal and annual Hg wet deposition for all stations, each backtrajectory was weighted according to its contribution to annual Hg deposition as a fraction of the total annual Hg deposition sum.

200 In other words, each of the 240 3D coordinates of each trajectory output was allocated a scalar value representing the measured Hg deposition value for that precipitation event. We then calculated the residence time of each weighed backtrajectory in 2° x 2° grid cells, with the fractional residence time in a particular grid cell based on the time of the entire trajectory. ~~For example, if a 10-day backtrajectory spent 12 hours of its time in a specific grid cell, it received a weighting of 5% for that particular grid cell.~~ The weighting of a backtrajectory residence time in a grid cell was then combined with the weighting of that trajectory as a fraction of total annual deposition, so that both the contribution to annual deposition as well as the residence time in grid cells were fully weighted. Finally, the sum of all backtrajectory weights for each grid cell were summed up and represented as a normalized frequency for each grid cell. We performed this both for 2014 Hg wet deposition, whereby the weighting occurred as the contribution of each trajectory to annual Hg wet deposition, and 2014-15 trace metal deposition. ~~Each weighted and normalized, 2° x 2° grid of values was finally converted to a raster file using the Python computing language package GDAL (PythonSoftwareFoundation;GDAL, 2016) and mapped and visualized in ArcGIS@.~~

3. Results and Discussion

3.1. Spatial, seasonal, and temporal patterns of Hg wet deposition concentrations

215 ~~We first present an analysis of concentration measurements of Hg and additional trace elements collected across the five deposition stations.~~ Minimum Hg concentrations at all stations were equal to the detection limit of the analyses (0.3 ng L⁻¹), and maximum concentrations strongly varied among stations. By far the highest Hg concentrations were reported for Gates of the Arctic with concentrations of up to 396 ng L⁻¹. ~~Our~~ Statistical analysis determined such high values as outliers, and ~~f~~, which is in agreement with other datasets that found background level concentrations generally ranging from 3 to 5 ng L⁻¹ (White et al., 2009) and considered elevated Hg concentrations (e.g., in central Illinois) when concentrations ranged above 20 ng L⁻¹ to 40 ng L⁻¹ (Lynam et al., 2014). For further analysis, we eliminated outlier concentrations (>26.14 ng L⁻¹) which we determined by an outlier analysis following the IQR rule

whereby (values above and below 1.5 x IQR were removed, 1.9% of all data). For consistency among the deposition stations, we selected a common outlier concentration across all stations, rather than delineate an outlier concentration for each station separately. ~~This outlier correction removed 1.9% of all data (17 values in total).~~ Median Hg wet deposition concentrations measured across the five deposition stations were in the following order, from highest to lowest (**Table 2**): Gates of the Arctic (3.6 ng L⁻¹) > Nome (3.5 ng L⁻¹) > Dutch Harbor (2.3 ng L⁻¹) > Kodiak Island and Glacier Bay (both 1.8 ng L⁻¹). The distribution of mean values followed the same general order (**Table 2**), although mean values were higher compared to median values due to skewed distribution in concentration data.

The highest wet Hg deposition concentrations (**Table 2**) were observed at the two northernmost sites Gates of the Arctic and Nome, with median values almost double and statistically higher compared to concentrations of the two lower latitude stations (Kodiak Island and Glacier Bay). A third station located at lower latitudes, Dutch Harbor, the westernmost station located on the Aleutian Islands, was similar in Hg concentrations as the two northern station and showed statistically higher concentrations (+28%) compared to the other two lower-latitude stations.

We determined that the major reason for higher Hg concentrations at northern sites was a lower dilution (or “wash-out” effect) of Hg concentrations by smaller storm sizes (**Figure 1** and discussion below). It is well-known that large precipitation events (i.e., bigger storms or increasing duration of storms) lead to lower Hg wet deposition concentrations compared to small events. ~~due This is due to~~ initially higher scavenging of airborne Hg, in particular of particulate-bound Hg (HgP) or gaseous oxidized Hg (GOM) (wash-out effect: Poissant and Pilote, 1998; Ferrara et al., 1986), ~~and has been observed in many studies~~ (Lamborg et al., 1995; Mason et al., 1997; Landis et al., 2002; Lyman and Gustin, 2008; Fain et al., 2011). Such “washout” effects also occurs in individual storms during which Hg concentrations are highest at the beginning of an event and decrease over time (Glass and Sorensen, 1999; Ferrara et al., 1986). However, ~~the a~~ washout effect cannot explain ~~the~~ higher Hg concentrations at Dutch Harbor which were similar to those at the more northern stations (see discussion below).

Figure 1a shows the presence of ~~the this~~ “washout” effect evident by inverse linear regressions between storm sizes (total weekly precipitation amounts) and respective measured weekly wet deposition Hg concentrations. All five stations showed statistically significant inverse correlations between the two variables. The slopes of the linear regressions, using log₁₀-transformed Hg concentrations (ng L⁻¹) and log₁₀-transformed precipitation (mm), varied between -0.28 and -0.46, but were not statistically different between stations (based on ANCOVA analyses). Overall, weekly precipitation totals explained 28% of the variability in Hg concentrations (r²=0.28, p-value<0.01, all sites). The common relationship between wet deposition concentrations and precipitation among all stations was best described by the following inverse linear relationship:

$$\log_{10}(Hg_{conc.}[ng L^{-1}]) = 0.844 - 0.347 \times \log_{10}(Precip[mm]) \quad (1)$$

Cumulative distribution of daily storm sizes (**Figure 1b**) show that higher precipitation amounts occurred at lower-latitude stations and were ~~a~~ driving factors leading to ~~their~~ lower wet deposition concentrations. For example, precipitation totals at Gates of the Arctic and Nome were three to five times lower compared to the three lower latitude sites. Similar to Hg concentrations, differences in precipitation totals were statistically significant between the northern and lower-latitude sites, but not between the two northern or among the three lower-latitude sites (based

on post-hoc comparison tests, not shown). The figure highlights a dominance of small precipitation events at Gates
260 of the Arctic and Nome, where a high fraction of precipitation events were below 1 mm. In comparison, the three
lower latitude sites experienced much higher fractions of daily storms, e.g., above 2 mm. We propose that the
washout effect largely accounts for higher Hg deposition concentrations at the dryer, northern sites compared to the
lower-latitude sites Glacier Bay and Kodiak Island. As mentioned, this analysis, however, fails to explain why
Dutch Harbor showed similarly high levels as the northern, more mesic sites.

265 **Figure 2** shows a pronounced seasonality of Hg wet deposition concentrations across all stations, with the highest Hg
concentrations in summers, followed by spring, winter, and fall. ANOVA analysis across all sites resulted in
statistically significant seasonal effects (variable “season”: $P < 0.01$), and post-hoc comparisons showed that Hg
concentrations differed among all seasons. ~~The ANOVA also showed that~~ Seasonal patterns were consistent among
270 the five stations with no significant differences among stations (i.e., no statistically significant interaction of “Season”
x “Station”). ~~Hence, seasonal patterns were relatively consistent among the five stations with~~ In general, median
concentrations ~~following~~ followed the order summer>spring>winter>fall, with one exception being Dutch Harbor
where fall concentrations were slightly above those in winter (2.0 ng L⁻¹ versus 1.9 ng L⁻¹).

Such seasonal patterns have been attributed to enhanced summertime GOM concentrations due to increased
275 photochemical formation of oxidized mercury in summer that leads to ~~increased atmospheric scavenging and~~ higher
Hg concentrations in precipitation (Pirrone and Mason, 2009; Selin and Jacob, 2008). ~~Yet, we propose found,~~
~~however,~~ that ~~observed~~ seasonal patterns ~~may also be~~ were affected by storm sizes and dilution effects since
precipitation amounts were generally lowest in summer and highest in fall and winter. We performed analysis on
seasonal differences by “detrending” data for different storm sizes, i.e., adjusting Hg concentrations by deducting the
280 linear trend of the washout effect (equation 1). ANOVA and post-hoc Bonferroni comparisons of detrended Hg
concentrations, however, showed that differences among seasons persisted after correcting for different precipitation
sizes per season, and that the order of Hg_{corr} concentrations followed the same order as the untrended concentrations
(summer > spring > fall/winter). Hence, we propose a combination of Hg oxidation processes (Pirrone and Mason,
2009; Selin and Jacob, 2008) along with precipitation sizes contributing to seasonal differences.

285 3.2. Spatial, seasonal, and annual patterns of Hg wet deposition loads

In order to calculate annual deposition loads, NADP MDN protocols ~~To calculate use annual wet deposition loads,~~
~~the MDN protocol uses multiplication of precipitation-weighted annual Hg concentration by annual precipitation~~
~~records for each station, and~~ require ~~substantial data coverage and stringent completeness criteria. These include,~~
290 that the percentage of valid Hg samples exceed 75%; the percentage for which precipitation amounts were available,
~~either from the rain gage or from the sample volume,~~ exceed 90%; and the percentage of total measured precipitation
associated with valid samples exceed 75%. ~~To calculate annual wet deposition loads, the MDN protocol uses~~
~~multiplication of precipitation-weighted annual Hg concentration by annual precipitation records for each station.~~
Following these constraints, data coverage allowed for a total of 16 years of annual wet deposition estimates across
the five stations (**Table 3**).

295 Annual Hg deposition values across the five stations averaged $3.55 \pm 1.48 \mu\text{g m}^{-2}$, with a minimum of $1.94 \mu\text{g m}^{-2}$ at
Gates of the Arctic in 2012 and a maximum of $5.74 \mu\text{g m}^{-2}$ at Kodiak Island in 2011. ~~In spite of differences in temporal
coverage of annual Hg deposition among stations, we observed consistent differences among sites. When data from
multiple stations were available,~~ The highest Hg deposition loads were always observed at Kodiak Island and lowest
at Gates of the Arctic, ~~and~~. Differences in wet Hg deposition loads between stations were large: for example, in the
300 four years of corresponding data, Kodiak Island deposition exceeded that at Dutch Harbor by a factor of 2.6 (in 2009),
2.4 (in 2011), 2.0 (in 2012), and 2.6 (in 2014). Second highest deposition loads were consistently observed at Dutch
Harbor, with loads that were slightly below those in Kodiak Island in the two years of corresponding measurements.
Statistical tests showed that annual deposition was statistically different among stations, and a post-hoc Bonferroni
comparison showed that this difference was driven largely by a statistically significant difference between the highest
305 (Kodiak Island) and lowest (Gates of the Arctic) station ($P < 0.05$). When using a statistical significance level of 10%
as opposed to 5%, we also observed significant differences between Kodiak Island and Glacier Bay and Kodiak Island
and Nome. Hence, ~~we generally can summarize~~ annual deposition loads ~~can be summarized~~ as follows: highest
deposition occurred at Kodiak Island ($4.80 \pm 1.04 \mu\text{g m}^{-2}$), but was not statistically different from ~~the second highest
station~~ Dutch Harbor ($4.52 \pm 1.47 \mu\text{g m}^{-2}$), but statistically different from all other stations. Lowest deposition was
310 observed at Gates of the Arctic ($2.11 \pm 0.67 \mu\text{g m}^{-2}$), and intermediate values were observed for Glacier Bay (3.00 ± 0.14
 $\mu\text{g m}^{-2}$) and Nome ($2.34 \mu\text{g m}^{-2}$). Although
~~Using all data and stations,~~ we did not observe significant effects of year of collection among stations ($P = 0.138$).
~~However, there,~~ we observed ~~was~~ substantial inter-annual variability in Hg deposition loads at individual stations.
For example, using the five years of measurements at Kodiak Island, values ranged from $3.14 \mu\text{g m}^{-2}$ (in 2009) to 5.61
315 $\mu\text{g m}^{-2}$ (in 2013), or a factor of 1.8 difference and a coefficient of variation of 22% (CV: Stdev/mean). The inter-
annual comparison of Gates of the Arctic showed values from $1.19 \mu\text{g m}^{-2}$ (2009) to $3.00 \mu\text{g m}^{-2}$ (2010), or a factor of
2.5 difference and a CV of 32% (Table 3). ~~Although the temporal coverage was too low to delineate clear inter-annual
trends, the available data record generally shows low deposition in 2009 when lowest deposition occurred both at
Gates of the Arctic and Kodiak Island. In the year 2011, generally high deposition was observed, with highest
deposition among all years observed at Dutch Harbor and Kodiak Island; however, the order of years was not fully
consistent among all stations.~~

Formatted: Tab stops: Not at 5.31"

3.2.1. Annual deposition loads and relationships to annual precipitation

In order to characterize what drives annual deposition loads, we analysed precipitation-weighted mean annual Hg
concentrations (PWM Hg) and annual precipitation, the two factors, which together constitute ~~the~~ annual deposition
325 load. Figure 3a shows a scatter plot and linear regression between PWM Hg and precipitation amounts using data of
all years and all stations (16 values), showing a strong linear relationship between PWM Hg and precipitation. The
regression slope explains 59% of the variability in PWM Hg, and a slope of -0.0189 suggests that with each 100 mm
increase in annual precipitation, PWM Hg concentration decreased on average by 1.9 ng L^{-1} . These patterns support a
strong dependence of Hg concentrations on precipitation ~~patterns~~ amounts, in agreement with the weekly Hg
330 concentration data showing ~~strong~~ dilution effects as discussed above. Yet, an important difference is that the annual

relationships between PWM Hg concentrations and precipitation is strongly linear, compared to non-linear functions between weekly Hg wet deposition concentrations and weekly precipitation (i.e., \log_{10} - \log_{10} relationships). The m
Figure 3a also shows that the range of annual precipitation is larger than the range of PWM Hg. For example, annual
total precipitation differed by almost a factor of 12 (lowest annual precipitation of 27 mm in 2013 at Gates of the
Arctic and highest precipitation of 316 mm at Kodiak Island in 2014). PWM Hg differed by a factor of 7 with lowest
concentration of 1.5 ng L⁻¹ in Glacier Bay in 2011 and highest concentrations of 10.0 ng L⁻¹ at Gates of the Arctic in
2010. When eliminating one unusually high PWM Hg concentration at Gates of the Arctic in 2010, the spread in PWM
Hg of the remaining 15 station years was further reduced to a factor of 4. This suggests that annual precipitation had
much stronger control in modulating annual deposition loads compared to PWM Hg concentrations. We conclude that
a major control in determining Hg wet deposition loads across the five Alaska station was is annual precipitation,
which alone explaineds 71% of the variability in observed annual deposition loads.

Compared to annual deposition observed across the contiguous U.S. (~~CONUS maps found at~~
~~<http://nadp.sws.uiuc.edu/mdn/>~~), Hg deposition in Alaska was extremely low. For example, Hg deposition across 99
deposition sites of the contiguous U.S. in 2014 averaged 9.7±3.9 μg m⁻², with a median value of 9.0 μg m⁻². compared
to Of the three Alaskan stations that allowed for calculation of annual Hg deposition loads in 2014, Gates of the
Arctic: (2.0 μg m⁻²), Kodiak Island (5.1 μg m⁻²), and Nome (2.4 μg m⁻²) where annual deposition was available for
2014, all showed very low deposition values compared to the other 99 U.S. stations. When comparing the multi-year
average annual Hg deposition of the Alaska stations to the 2014 deposition values across the contiguous U.S. in 2014,
three Alaska stations (Nome: 2.3 μg m⁻², Glacier Bay: 3.0 μg m⁻², Gates of the Arctic: 2.1 μg m⁻²) showed annual
deposition below all of the lower 48 contiguous U.S. States in 2014 (lowest value in the contiguous U.S. of 3.1 μg m⁻²
observed at CA94, Converse Flats San Bernardino). Only Dutch Harbor (4.5 μg m⁻²) and Kodiak Island (4.8 μg m⁻²)
exceeded the lowest deposition loads of the lower 48 States, yet even these two stations fell below the 5th percentile
of annual deposition observed at the 99 lower 48 States in 2014 (5.3 μg m⁻²).

Similarly, PWM Hg concentrations were very low in Alaska compared to the rest of the U.S., which for the year 2014
averaged 10.6±9.1 ng L⁻¹ with a median value of 8.9 ng L⁻¹. Three Alaskan stations showed annual PWM Hg
concentrations below the minimum concentrations (3.0 ng L⁻¹) of any of the stations in the contiguous United States,
including Dutch Harbor (2.9 ng L⁻¹), Glacier Bay (1.9 ng L⁻¹), and Kodiak Island (2.2. ng L⁻¹). Nome with an annual
PWM concentration of 6.2 ng L⁻¹ and Gates of the Arctic (6.0 ng L⁻¹) were below the 15th percentile of concentrations
of the lower 48th States. We conclude that low deposition values observed across coastal regions in Alaska were driven
largely by very low wet deposition concentrations below concentrations at any of the contiguous U.S. deposition
stations. For the two northern stations, Gates of the Arctic and Nome, extremely low wet Hg deposition was driven
by a combination of low deposition concentrations and very low annual precipitation.

Overall, vIn summary, very low concentrations and deposition totals were observed throughout Alaska, typical of very
remote areas with few local or regional point sources and representative of more large-scale global background
circulation patterns. It is important, however, to note that wet deposition as reported in this study constitutes only part
of the total Hg deposition. In terrestrial ecosystems, there is ample evidence that dry deposition of Hg constitutes a
major Hg source, in large parts including gaseous elemental Hg which account for 57-94% of Hg found in soils (Obrist

Formatted: Font: Not Bold

Formatted: Not Superscript/ Subscript

Formatted: Not Superscript/ Subscript

et al., 2018). This evidence is based stable Hg isotope studies (e.g., Demers, Blum et al. 2013 and subsequent studies) along with earlier forest studies that showed that litterfall and throughfall deposition dominate as major dry deposition sources in forests (e.g., Iverfeldt 1991, Munthe, Hultberg et al. 1995). In Alaska, a recent study in the northern Tundra (Obriest et al., 2017) showed that wet deposition accounted for a minor fraction of overall Hg deposition, with the largest source to the tundra deriving from atmospheric gaseous Hg deposition cycled through arctic vegetation.

3.2.2. Spatial scaling of Hg deposition to the entire State of Alaska

We used spatial interpolation and extrapolation techniques to create maps of deposition concentrations and deposition loads across the state of Alaska, following interpolation protocols described by the National Atmospheric Deposition Program (NADP, 2016). Limitations of such deposition maps, as stated by the NADP network, include: that “stations and maps represent regional trends (rather than local sources); that uncertainty with maps varies geographically, have not been quantified, and high levels of uncertainty can occur due to topographic variability, near urban and industrial areas, and in regions isolated from deposition sites”. The NADP network specifically cautions making decisions based on projected maps when no direct measurements are available. For estimation of spatial deposition maps (i.e., sum of deposition, seasonal and annual deposition loads), we did not remove values associated with outlier Hg concentrations and we included all officially released annual MDN deposition data that were quality controlled following official MDN protocols. In any case, because outliers were always associated with very low precipitation amounts, removal of outlier Hg concentrations have extremely small impacts on annual deposition loads. Concentration maps shown in Figure 4 are based on the inverse distance weighting interpolation method of average PWM Hg concentrations for each station (Figure 4a), and as such represents different collection years and number of years for each station based on the available data set. For example, the maps are based on 2 years (2011 and 2012) of wet Hg deposition data for Dutch Harbor, 1 year (2014) for Nome, two years (2011 and 2012) for Glacier Bay, five years (2009–2014 without 2013) for Gates of the Arctic, and six years (2008–2014 without 2010) for Kodiak Island.

The resulting Hg concentration maps (shown in Figure 4) present a coarse spatial representation of the concentrations patterns (i.e. only five measurement stations) that relate to precipitation gradients, with the highest concentrations observed at the northern two stations that show low annual precipitation and small storm sizes. The use of inverse weighting procedures result in interpolation of Hg concentrations that are were not fully in accordance with the observed relationships to precipitation patterns. For example, precipitation maps show strong gradients in annual precipitation from the southern coast of Alaska to inland and northern locations, and relatively consistently low precipitation values across much of central, northern, and eastern Alaska. In contrast, the interpolated Hg concentration map shows that interior and eastern Alaskan concentrations follow north-to-south gradients between the lower-latitude and higher-latitude stations, but do not account for east-west gradients. While we could have used precipitation-based estimates of Hg concentrations across the State (based on strong relationships of PWM Hg and annual precipitation), we decided not to deviate from common NADP mapping procedures.

Figure 4b shows precipitation maps across Alaska based on precipitation data averaged for the years 2007 to 2015. The long-term NOAA precipitation maps show strong gradients from the southern coastal locations to interior and

Commented [OD5]: Obriest, D., J. L. Kirk, L. Zhang, E. M. Sunderland, M. Jiskra and N. E. Selin (2018). "A review of global environmental mercury processes in response to human and natural perturbations: Changes of emissions, climate, and land use." *Ambio* 47(2): 116-140.

Commented [OD6]: Demers, J. D., J. D. Blum and D. R. Zak (2013). "Mercury isotopes in a forested ecosystem: Implications for air-surface exchange dynamics and the global mercury cycle." *Global Biogeochemical Cycles* 27(1): 222-238.

Commented [OD7]: Iverfeldt, Å. (1991). "Mercury in forest canopy throughfall water and its relation to atmospheric deposition." *Water, Air, and Soil Pollution* 56: 553-564. Munthe, J., H. Hultberg and Å. Iverfeldt (1995). "Mechanisms of deposition of methylmercury and mercury to coniferous forests." *Water Air and Soil Pollution* 80(1-4): 363-371.

Commented [OD8]: Obriest, D., Y. Agnan, M. Jiskra, C. L. Olsen, D. P. Colegrove, J. Hueber, C. W. Moore, J. E. Sonke and D. Helmig (2017). "Tundra uptake of atmospheric elemental mercury drives arctic mercury pollution." *Nature* 547: 201-2014.

405 northern Alaska, with very strong precipitation changes within short distance (50-100 miles). The highest annual
precipitation was observed along the southeastern and southcentral coasts, with maximum precipitation of
approximately 610 cm yr⁻¹, and high precipitation amounts in the range of (200 to 300 cm yr⁻¹) were also observed
in Kodiak Island and Bristol Bay and the Aleutian/Probilof Islands. Moderate precipitation was observed in the
410 southcentral and southwestern region of Alaska, generally in the range of 100 to 200 cm yr⁻¹, whereby occasionally
higher levels of precipitation were observed in the mountain regions due to orographic precipitation effects. In the
interior and far north regions of Alaska, however, annual precipitation sums were low and generally below 100 cm yr⁻¹.

The resulting annual Hg deposition maps, i.e., the product of annual Hg_{pw} concentrations and precipitation, are shown
in **Figure 4c**. Based on this map, we projected distinct zones of highest Hg deposition in Alaska along the southern
and southeastern coasts, with annual Hg deposition exceeding 20 µg m⁻² yr⁻¹. The zones of highest annual Hg
415 deposition, based on the estimated map, however, were confined to narrow zones of approximately 50-100 miles
inland. Similarly, high Hg deposition may have occurred in isolated mountain areas near the southern coast such as in
the Alaskan Range. For example, in the Denali National Park Region, estimated Hg wet deposition of up to 15 µg m⁻²
yr⁻¹ was in a similar magnitude of the highest deposition amounts along the southern and southeastern coast. Lower
Hg deposition amounts were projected, and in fact observed, along the southwestern coastal region, including Kodiak
420 Island and the western and eastern Aleutians. Here, estimated annual Hg deposition were in the range 5 to 10 µg m⁻²
yr⁻¹. Our estimated deposition maps indicated that in much of the State of Alaska, in particular in the interior and far
northern regions, Hg deposition was very low, with annual Hg deposition generally below 4 µg m⁻² yr⁻¹ and in many
areas (e.g., north of the Brooks Range) only in the range of 1-2 µg m⁻² yr⁻¹.

As stated above, estimated maps of estimated annual deposition need to should be considered with caution as they are
425 based on interpolation methods and may include a variety of possible errors. Compared to measured deposition at the
five stations, estimated deposition fell well within 10% of observations at Gates of the Arctic and Kodiak Island. At
other stations, we found larger discrepancies between observed and modelled deposition, and at Glacier Bay and Nome
discrepancies were over 100%. We attributed these larger biases to discrepancies in annual precipitation: for example,
at Glacier Bay and Nome, the model strongly overestimated precipitation (by 90% and 117%, respectively) which
430 accounted for the main part of the bias. Reasons for precipitation errors were mainly due to the large grid size of the
modelled precipitation combined with strong coastal gradients. For example, the deposition station at Glacier Bay,
which was situated close to Point Gustavus in the inner Bay about 50 km inland from the main coast, was located
along a very large precipitation gradient which was not appropriately resolved by the grid size of the precipitation
maps. Another possible reason for differences between observed and predicted deposition may include issues of
435 precipitation fetch during deposition measurements. Precipitation gages generally show a strong bias towards under-
catch of precipitation caused by wind, even with precipitation gauges that are designed with wind protection (Savina
et al., 2012; Yang et al., 2000). Snowfall, which accounts for a very important fraction of annual precipitation in this
area, can lead to under-catch ranging from 20 to 50% during windy conditions (Rasmussen et al., 2012).

3.2.3. Back-trajectory determine source regions of Hg deposition

440 We performed comprehensive back-trajectory analyses for the year 2014 which represented a typical deposition year and included data from the station with highest (Kodiak Island), lowest deposition (Gates of the Arctic) and intermediate (Nome) deposition amounts stations. As described in the methods section, individual backtrajectory modelling was performed for all individual precipitation events (total of 247 events for Kodiak Island, 182 events for Nome, and 148 events for Gates of the Arctic) and subsequently each deposition event was weighted by its contribution to annual deposition load. Finally, we summarized residence times of all backtrajectories for all 0.5 x 0.5 degree grid cells. Figure 5 shows normalized backtrajectory frequency maps for annual precipitation (panels a to c) and Hg deposition (panels d to f) for the year 2014.

445 For Kodiak Island, trajectory frequency maps showed almost identical patterns for precipitation and Hg deposition, both indicating the highest trajectory frequencies in close vicinity of the deposition station and to the south of the station. These patterns were attributed to the fact that each trajectory passed through adjacent station grid cells prior to arriving at the deposition station so that the vicinity of the stations always showed high contributions (both for precipitation and Hg deposition). In addition, major source origins for both precipitation and Hg wet deposition stemmed from the Gulf of Alaska with additional contributions further south in the eastern Pacific Ocean up to a distance of 2,500 km south of Kodiak Island. A similar pattern was observed for Gates of the Arctic where close agreements existed between source origins of precipitation and Hg deposition. Where high contributions to annual Hg deposition and precipitation were observed again in the vicinity of the station, with additional source regions from the center of the Bering Sea and the Gulf of Alaska. There were only a few occasions where storms or deposition events were tracked far into the western Pacific. We conclude that Gates of the Arctic experienced similar source regions for precipitation and Hg deposition and that these were predominantly located in the Bering Sea and the Gulf of Alaska.

460 A different pattern was evident for Nome. Here, the frequency distributions of trajectories differed between precipitation and Hg wet deposition. Precipitation showed high source regions in the vicinity of the station and also relatively wide distribution across the Bering Sea, the central Pacific, and the western Pacific. For Hg, showed increased contributions, relative to that of precipitation, were clearly visible in the western Pacific downwind of East Asia, indicating This pattern indicated significant contributions from east Asia where known high Hg emission sources such as mining, industrial emissions, and coal burning have led to increased atmospheric Hg levels (Wong et al., 2006). A recent study by Pacyna et al. (2016), identified east Asia and India as the dominant source areas of global anthropogenic Hg emission from 2005 to 2010. Evidence that Hg pollution in East Asia contributes to elevated wet deposition Hg levels in downwind areas are also seen by the recently established Asia-Pacific Mercury Monitoring Network (APMMN) where preliminary data shows average wet deposition concentrations ranging from 7 to 23 ng L⁻¹ in samples covering areas from Vietnam to Korea (Sheu, 2017).

3.3. Auxiliary trace metal concentrations at Dutch Harbor (AK00), Kodiak Island (AK98), and Nome (AK04)

475 Across the three stations with data and deposition samples, we found the following order of median concentrations (MLE-based) of trace elements (Table 4): Zn ($1.40 \mu\text{g L}^{-1}$) > As ($0.19 \mu\text{g L}^{-1}$) > Cu ($0.14 \mu\text{g L}^{-1}$) > Se ($0.06 \mu\text{g L}^{-1}$) > Ni ($0.04 \mu\text{g L}^{-1}$) > Pb ($0.04 \mu\text{g L}^{-1}$) > Cr ($0.02 \mu\text{g L}^{-1}$) > Hg ($0.002 \mu\text{g L}^{-1}$). Highest concentrations were always observed for Zn which exceeded concentrations of all other elements by over an order of magnitude. Similarly, by far the lowest concentrations were always observed for Hg which was below concentrations of all other trace metals by at least one order of magnitude. Similar patterns of trace element concentrations, although generally higher in concentrations, have been observed in snow samples at lower latitudes, such as in Utah snowpack where Carling et al. (2012) observed highest bulk (unfiltered) concentrations of Zn in the range of $3\text{--}4 \mu\text{g L}^{-1}$, with concentrations that exceeded that of other trace metals several-fold, and similarly, Hg concentrations were about one order of magnitude below concentrations of other trace elements. In the Everest region in the Himalayas, Lee et al. (2008) observed high concentrations of Zn ($0.48 \mu\text{g L}^{-1}$) as well compared to other trace elements (e.g., 0.11 for Cr, 0.08 for Pb and Ni, 0.01 for As). Here, concentrations were in a similar range as those observed in Alaska. In fresh snow in the French Alps, Veysseyre et al. (2001) observed concentrations of Zn up to $0.75 \mu\text{g L}^{-1}$, again the highest compared to other trace metals (e.g., up to Cu: $0.2 \mu\text{g L}^{-1}$) although Pb showed some high values in that study as well (max. of $1.76 \mu\text{g L}^{-1}$).

490 An outlier analysis using the 1.5x IQR rule identified only a few points as outliers, i.e., only 1 or 2 for Se, Cr, Zn, Hg to a maximum of 6 for As. Similar to Hg, outlier concentrations were observed mainly at very low precipitation amounts, suggesting quality issues when low amounts of wet deposition were collected. For example, median precipitation of outlier data (all elements) was 0.46 cm, while the median precipitation of all samples was 2.7 cm. Therefore, we find evidence that at low precipitation, quality issues exist with trace metal samples, possibly due to blank values that result in unusually high concentrations at low precipitation. For further analysis and statistics, we therefore chose to remove outlier concentrations as many statistical tests are sensitive to such outliers.

3.3.1. Principal component analyses of the full trace element concentration dataset

500 In this section, we use Principal Component Analysis (PCAs) to explore commonalities of trace metals using both the entire dataset available across the three stations as well as individual stations. According to Reimann et al. (2008), large geochemical datasets can use PCA to graphically inspect and reduce the data into a few components that may explain a high amount of the variability of the complete data.

Figure 6 shows PCAs using all elements for all sites (panel a) and for each individual site separately (panels b-d), with a graphical representation showing the two main components (first component: x-axis; second component: y-axis). Similar patterns appeared in both the all data PCA and the individual site analyses. All elements showed a strong negative correlation with component one, suggesting that all element concentrations increased and decreased together.

505 Component 1 likely represents precipitation with washout effects leading to lower chemical concentrations with larger storms. Interestingly, Hg showed the weakest correlation with component one, possibly related to Hg's highly volatile nature relative to other trace metals.

Formatted: Normal, Line spacing: single

Ni, Cr, and Hg consistently fell on the negative side of the second component, while Pb and As fell on the positive side of the second component. Weaker associations were observed for Se, Pb, and As. We propose that the 2nd principal component may represent differences in the trace metals origins. Ni and Cr were likely associated because of a common source profile, possibly linked due to a similar crustal and/or natural sources (Carling et al., 2012; Agnan et al., 2015b; Veysseyre et al., 2001). On the opposite loading of this second principal component we found Pb and As, possibly due to their different source origins. As and Pb are primarily driven by anthropogenic, industrial emission sources such as smelters and combustion processes (Tchounwou et al., 2012), and these may in some part be derived from long-range transport from Asia. Hg's association with Ni and Cr supports a more background/natural source rather than local or point driven pollution source, or its distinctly different atmospheric behaviour due to its presence in gaseous phase.

It is possible, however, that a portion of the factor loadings are related to site differences, as we did not find fully consistent patterns of elements across different sites. As discussed above, we observed that (i) all elements were statistically higher in concentrations at Nome compared to Kodiak Island; (ii) all elements except Pb and Se were statistically higher at Nome compared to Dutch Harbor; and (iii) only As, Pb, and Se were statistically higher at Dutch Harbor compared to Kodiak Island. It was therefore possible that factor 2 may reflect a different spatial distribution of As, Pb, and Se compared to most other elements (or particularly to Ni and Cr). Yet, analysis at individual sites (Figure 6 panels b to d) showed that the separation along component 2 was consistent across all sites. Hence, the pattern was consistent across all three sites with strong loading of Ni and Cr on one side of the second component and the opposite loading of As and Pb.

3.3.2. Enrichment factors of trace elements to assess geogenic (dust) and other sources including anthropogenic contributions

Further information about natural (geogenic/dust) versus anthropogenic sourcing sources were may be derived from calculations of enrichment factors. The calculation of enrichment factors of upper continental crustal distribution, (EF_{UCC}), showed ratios of elements of interest to a conservative crustal element such as Al. Al is a good tracer for crustal and rock elements and contributions from dust deposition. Using normalized ratios of other elements to that of upper continental crust (Wedepohl, 1995), the method calculates enrichments of elements above what is would be expected from purely natural sources. Enrichment factors were calculated following equation 3 (e.g., Carling et al., 2012):

$$EF_{UCC} = \frac{X_{i,s} / \sum_{j=1}^n X_{j,s}}{X_{i,UCC} / \sum_{j=1}^n X_{j,UCC}} \quad (2)$$

Unfortunately, the dataset on Alaska wet deposition did not have data for Al nor other elements commonly used as conservative geogenic tracers such as Ti or Fe. In order to still perform calculations of enrichment factors, we decided to use Cr and Ni instead as two possible reference elements. Both of these elements often show low enrichment factors compared to Al, indicating mainly crustal origins as for Al (Carling et al., 2012; Agnan et al., 2015b; Veysseyre et al., 2001). Uncertainties in this methodology include that local or regional soil elemental composition can be different from used reference crustal composition.

Formatted: Strikethrough

- Formatted: Strikethrough
- Formatted: Strikethrough
- Formatted: Strikethrough
- Formatted: Strikethrough
- Formatted: Strikethrough
- Formatted: Strikethrough
- Formatted: Strikethrough
- Formatted: Strikethrough
- Formatted: Strikethrough
- Formatted: Strikethrough
- Formatted: Strikethrough
- Formatted: Strikethrough
- Formatted: Strikethrough
- Formatted: Strikethrough
- Formatted: Strikethrough
- Formatted: Strikethrough
- Formatted: Strikethrough
- Formatted: Strikethrough

545 Calculated EF_{wec} are shown in **Figure 7** for all data from all three stations. EF_{wec} between 0.1 to 10 indicated that dominant sources were from soils, dust, or rocks; high EF_{wec} values were indicative of other natural or anthropogenic sources, whereby ratios between 10 to 500 were moderately enriched and values above 500 were strongly enriched and indicative of anthropogenic contributions (Lee et al., 2008; Carling et al., 2012). Based on this, we would classify Cr, Pb, and Ni with median values below 10 as primarily derived from crustal contributions. The only element we would clearly characterize as strongly enriched compared to crustal composition was Se with a median EF_{wec} of 1054. Moderately enriched EF_{wec} factors were observed for Cu, As, Zn, and Hg, with EF_{wec} values ranging from 11 to 57. **Figure 7** shows that the range and order of EF_{wec} was very consistent among the three stations, always showing a separation of elements with distinctly different EF_{wec} values: low values for Cr, Pb, and Ni, median ranges for Cu, As, Zn, and Hg, and the highest value for Se.

550 This analysis ~~suggested~~ suggests that the clustering of the elements Cr and Ni in the PCA analysis above was in fact likely driven by a common crustal origin. The results ~~were~~ are also in support of the possibility that the opposite loading on the second principal component for Se and As could in part be driven by other sources (e.g., natural sources such as an ocean source for Se (Amouroux et al., 2001) or anthropogenic sources for As. For Pb, in contrast to PCA results, low EF_{wec} ~~suggested~~ suggests crustal sources similar to Cr and Ni. We conclude that enrichment factors for Cr and Ni were showing low enrichment factors in support of predominantly crustal sources, while high enrichment factors for Pb and Se ~~suggested~~ suggests additional anthropogenic and natural sources. For most other elements, including Hg, enrichment factors ~~fell~~ were in between, ~~indicating no clear~~ not indicating clear crustal or anthropogenic ~~source signature~~.

4. Conclusions

565 Our analysis of wet deposition data from five stations in Alaska found that Hg concentrations in precipitation at the two northern stations (Nome and Gates of the Arctic) were consistently and significantly higher than the two lowest-latitude sites (Kodiak Island and Glacier Bay). These differences were largely explained by different precipitation regimes, with high amounts of precipitation at the lower latitude stations leading to washout effects compared to dryer, northern deposition sites. Differences in Hg concentrations between sites still existed after the effects of precipitation differences were removed, ~~although the influence of precipitation was strong. After the correction, with~~ Gates of the Arctic (AK06) and Nome (AK04) ~~still had showing~~ the highest Hg concentrations in precipitation and Kodiak Island statistically still had the lowest Hg concentrations, ~~which~~ This suggested suggests that other factors contributed to ~~higher-observed differences in~~ Hg concentrations in wet deposition at these stations as well.

575 Highest annual Hg deposition loads were always observed at Kodiak Island (AK98), and lowest deposition loads were always observed at Gates of the Arctic (AK06), and these differences were substantial. For example, Kodiak Island (AK98) exceeded deposition at Dutch Harbor (AK00) by a factor 2.64 (in 2009), 2.40 (in 2011), 2.10 (in 2012), and 2.55 (in 2014). These patterns also were explained to a large degree by precipitation differences, ~~whereby a~~ Across all stations and collection years, precipitation overwhelmingly controlled annual Hg deposition ~~and~~ annual precipitation ~~alone~~ explained 73% of the variability in observed annual Hg deposition ~~across all stations and monitoring years. In comparison to Hg deposition loads across the contiguous United States, our analyses revealed that a~~ Annual Hg deposition loads for all of Alaska were among the lowest anywhere in the United States falling into

Formatted: Strikethrough

Formatted: Strikethrough

Formatted: Strikethrough

Formatted: Strikethrough

Commented [OD9]: Remove?

580 the lowest 5th percentile of all observed annual deposition. Based on observations and spatial interpolations, we found distinct zones of highest-higher Hg deposition in Alaska along the southern and southeastern coasts (confined to 50-100 miles inland), and similarly high Hg depositions in isolated mountain areas near the southern coast, due to orographic precipitation enhancement. Lower Hg deposition amounts were observed along the southwestern coastal region, including Kodiak Island and the western and eastern Aleutians. For most of the state, particularly in the interior and far northern regions, Hg deposition were estimated to be very low.

585 Back trajectory analysis of 2014 deposition data showed almost identical source origins of precipitation and Hg wet deposition, suggesting that the origin of Hg deposition was closely related to the origin of precipitation at the largely diffuse and regional Hg sources at Gates of the Arctic (AK06) and Kodiak Island (AK98). Conversely, origins of precipitation and Hg wet deposition at Nome (AK04) were quite different; with for Hg deposition, we found increased source contributions relative to that of precipitation in the western Pacific Ocean near the East Asian continent, possibly, which could be due to long-range transport from East Asian emissions.

PCA analyses revealed two distinct associations of trace elements: Cr and Ni were clustered, and so were As and Pb, which were attributable to different source origins. Sources of Ni and Cr are often considered driven by crustal (e.g., dust) sources, while As and Pb are attributable to anthropogenic inputs, including by long-range transport from Asia.

595 Mercury, nor any of the other trace elements analysed, did not consistently associate with any of these four elements, suggesting more diffuse and possibly different source origins or a distinctly different behaviour in the atmosphere for these elements. Calculations of enrichment factors (i.e., elemental enrichment compared to the upper continental crust) showed low enrichment factors for Cr and Ni in support of predominantly crustal sources, while high enrichment factors for Pb and Se suggested suggests additional anthropogenic and natural sources. For most other elements, including Hg, enrichment factors were in between these elements, not indicating a clear attribution to either crustal or anthropogenic source origins.

600 Based on our findings, we recommend continued monitoring of Hg wet deposition at select sites designed to capture the strong precipitation gradients observed throughout Alaska. Given the low wet deposition amounts of Hg across most of Alaska, we recommend additional focus on dry deposition monitoring, as recent research has suggested suggests that deposition of gaseous elemental Hg (Hg^0) dominates Hg loading in most arctic tundra terrestrial ecosystems and across other vegetated ecosystems (Obrist et al., 2017, 2018, Jiskra et al., 2018). Finally, gAdditional collection and analysis of typical source tracers (e.g., Fe, Al, or Ti for dust; Cl, Na, Mg for ocean sources; gaseous tracers such as CO, CO₂, and O₃ as combustion tracers; ²²²Rn as a boundary layer tracer) may help facilitate better source apportionment both for wet deposition as well as for gaseous species (e.g., Hg^0). Global warming is a particular concern in northern latitudes, with warming occurring at a rate almost twice the worldwide average in the Arctic (Polyakov et al., 2002). Global warming will change precipitation patterns and associated deposition dynamics, including shortening of winter and changes in the fraction of snow and rain. In addition, climate change will have profound consequences on other ecosystem processes, including loss of permafrost and increased active layer depths of soils of (Schuur et al., 2008) and profound changes in hydrology (Vonk et al., 2015a), with complex, yet poorly understood, consequences on exposure to Hg (Obrist et al., 2018).

Commented [OD10]: Obrist, D., et al. (2018). "A review of global environmental mercury processes in response to human and natural perturbations: Changes of emissions, climate, and land use." *Ambio* 47(2): 116-140.
Obrist, D., et al. (2017). "Tundra uptake of atmospheric elemental mercury drives arctic mercury pollution." *Nature* 547: 201-2014.
Jiskra, M., et al. (2018). "A vegetation control on seasonal variations in global atmospheric mercury concentrations." *Nature Geoscience* 11(4): 244-250.

Commented [OD11]: Polyakov IV, Alekseev GV, Bekryaev RV, Bhatt U, Colony RL, Johnson MA, et al. Observationally based assessment of polar amplification of global warming. *Geophys. Res. Letters* 29, 1878 (2002).
18. ACIA, "Impacts of a warming Arctic: Arctic Climate Impact Assessment. ACIA Overview report" (Cambridge University Press, 2004).

Formatted: Font: 10 pt

Commented [OD12]: Schuur, E. A. G., B. Abbott, and N. Permafrost Carbon (2011), High risk of permafrost thaw. *Nature*, 480(7375), 32-33.

Commented [OD13]: Vonk JE, Tank SE, Bowden WB, Laurion I, Vincent WF, Alekseychik P, et al. Reviews and syntheses : Effects of permafrost thaw on Arctic aquatic ecosystems. *Biogeosciences* 2015; 12: 7129-7167.

Formatted: Check spelling and grammar

5. Author Contributions

CP and DO designed this analysis. CP analysed the data and generated figures. DH performed the HYSPLIT backtrajectory modelling. CP and DO prepared the manuscript with contributions from all co-authors.

6.5. Acknowledgements

This work was funded by the Alaska Department of Environmental Conservation Grant #: USFSW/15.668/F12AF00730. Funding was also provided by a collaborative research project by the U.S. National Science Foundation (Award #1739567 and 1304305).

7.6. References

Ackerman, J. T., Eagles-Smith, C. A., Herzog, M. P., Hartman, C. A., Peterson, S. H., Evers, D. C., Jackson, A. K., Elliott, J. E., Vander Pol, S. S., and Bryan, C. E.: Avian mercury exposure and toxicological risk across western North America: a synthesis, *Sci Total Environ*, <http://dx.doi.org/10.1016/j.scitotenv.2016.03.071>, 2016.

Agnan, Y., LeDantec, T., Moore, C., Edwards, G., and Obrist, D.: New constraints on terrestrial surface-atmosphere fluxes of gaseous elemental mercury using a global database, *Environ Sci Technol*, 19, 507-524, 2015a.

Agnan, Y., Sejalon-Delmas, N., Claustres, A., and Probst, A.: Investigation of spatial and temporal metal atmospheric deposition in France through lichen and moss bioaccumulation over one century, *Sci Total Environ*, 529, 285-296, [10.1016/j.scitotenv.2015.05.083](http://dx.doi.org/10.1016/j.scitotenv.2015.05.083), 2015b.

AMAP: AMAP Assessment 2002: Heavy Metals in the Arctic, Arctic Monitoring and Assessment Programme (AMAP), Oslo, Norway, xvi + 265 pp., 2005.

AMAP: Assessment 2009: Human Health in the Arctic, Oslo, Norway, 2009a.

AMAP: Arctic Pollution 2009, Arctic Monitoring and Assessment Programme (AMAP), Oslo, Norway, 83, 2009b.

AMAP: Arctic Pollution 2011, Arctic Monitoring and Assessment Programme (AMAP), Oslo, Norway, 38, 2011.

Amouroux, D., Liss, P. S., Tessier, E., Hamren-Larsson, M., and Donard, O. F.: Role of oceans as biogenic sources of selenium, *Earth and Planetary Science Letters*, 189, 277-283, 2001.

Baeyens, W., Leermakers, M., Papina, T., Saprykin, A., Brion, N., Noyen, J., De Gieter, M., Elskens, M., and Goeyens, L.: Bioconcentration and biomagnification of mercury and methylmercury in North Sea and Scheldt estuary fish, *Arch Environ Con Tox*, 45, 498-508, DOI [10.1007/s00244-003-2136-4](https://doi.org/10.1007/s00244-003-2136-4), 2003.

Bocharova, N., Treu, G., Czirják, G. Á., Krone, O., Stefanski, V., Wibbelt, G., Unnsteinsdóttir, E. R., Hersteinsson, P., Schares, G., Doronina, L., Goltsman, M., and Greenwood, A. D.: Correlates between Feeding Ecology and Mercury Levels in Historical and Modern Arctic Foxes (*Vulpes lagopus*), *PLoS ONE*, 8, e60879, [10.1371/journal.pone.0060879](https://doi.org/10.1371/journal.pone.0060879), 2013.

Braune, B. M., Gaston, A. J., Gilchrist, H. G., Mallory, M. L., and Provencher, J. F.: A geographical comparison of mercury in seabirds in the eastern Canadian Arctic, *Environ. Int.*, 66, 92-96, [10.1016/j.envint.2014.01.027](https://doi.org/10.1016/j.envint.2014.01.027), 2014.

Brockhoff, C., Creed, J., Martin, T., Martin, E., and Long, S.: EPA Method 200.8, Revision 5.5: Determination of trace metals in waters and wastes by inductively coupled plasma-mass spectrometry, EPA-821R-99-017, 1999.

Brunke, E. G., Labuschagne, C., and Slemr, F.: Gaseous mercury emissions from a fire in the Cape Peninsula, South Africa, during January 2000, *Geophysical Research Letters*, 28, 1483-1486, 2001.

Carling, G. T., Fernandez, D. P., and Johnson, W. P.: Dust-mediated loading of trace and major elements to Wasatch Mountain snowpack, *Sci Total Environ*, 432, 65-77, [10.1016/j.scitotenv.2012.05.077](https://doi.org/10.1016/j.scitotenv.2012.05.077), 2012.

Dietz, R., Outridge, P. M., and Hobson, K. A.: Anthropogenic contributions to mercury levels in present-day Arctic animals-A review, *Sci Total Environ*, 407, 6120-6131, DOI [10.1016/j.scitotenv.2009.08.036](https://doi.org/10.1016/j.scitotenv.2009.08.036), 2009.

Dommergue, A., Sprovieri, F., Pirrone, N., Ebinghaus, R., Brooks, S., Courteaud, J., and Ferrari, C. P.: Overview of mercury measurements in the Antarctic troposphere, *Atmos. Chem. Phys.*, 10, 3309-3319, [10.5194/acp-10-3309-2010](https://doi.org/10.5194/acp-10-3309-2010), 2010.

- Douglas, T. A., and Sturm, M.: Arctic haze, mercury and the chemical composition of snow across northwestern Alaska, *Atmospheric Environment*, 38, 805-820, 2004.
- Douglas, T. A., Loseto, L. L., Macdonald, R. W., Outridge, P., Dommergue, A., Poulain, A., Amyot, M., Barkay, T., Berg, T., Chetelat, J., Constant, P., Evans, M., Ferrari, C., Gantner, N., Johnson, M. S., Kirk, J., Kroer, N., Larose, C., Lean, D., Nielsen, T. G., Poissant, L., Rognerud, S., Skov, H., Sorensen, S., Wang, F., Wilson, S., and Zdanowicz, C. M.: The fate of mercury in Arctic terrestrial and aquatic ecosystems, a review, *Environmental Chemistry*, 9, 321-355, 10.1071/en11140, 2012.
- 665 Dray, S., and Dufour, A. B.: The ade4 package: implementing the duality diagram for ecologist, *Journal of Statistical Software*, 22, 1-20, 2007.
- 670 Eagles-Smith, C. A., Ackerman, J. T., Willacker, J. J., Tate, M. T., Lutz, M. A., Fleck, J. A., Stewart, A. R., Wiener, J. G., Evers, D. C., Lepak, J. M., Davis, J. A., and Pritz, C. F.: Spatial and temporal patterns of mercury concentrations in freshwater fish across the western United States and Canada. , *Sci Total Environ*, <http://dx.doi.org/10.1016/j.scitotenv.2016.03.229>, 2016.
- 675 U.S. Environmental Protection Agency: Initial List of Hazardous Air Pollutants with Modifications: <https://www.epa.gov/haps/initial-list-hazardous-air-pollutants-modifications>, 2016.
- U.S. EPA Toxics Release Inventory 2014: <https://www.epa.gov/toxics-release-inventory-tri-program>, access: 08/27/2016, 2014.
- Evans, M. S., Lockhart, W. L., Doetzel, L., Low, G., Muir, D., Kidd, K., Stephens, G., and Delaronde, J.: Elevated mercury concentrations in fish in lakes in the Mackenzie River Basin: The role of physical, chemical, and biological factors, *Sci Total Environ*, 351, 479-500, DOI 10.1016/j.scitotenv.2004.12.086, 2005.
- 680 Faïn, X., Obrist, D., Pierce, A., Barth, C., Gustin, M. S., and Boyle, D. P.: Whole-watershed mercury balance at Sagehen Creek, Sierra Nevada, CA, *Geochim. Cosmochim. Acta*, 75, 2379-2392, 2011.
- Ferrara, R., Maserti, B., Petrosino, A., and Bargagli: Mercury levels in rain and air and the subsequent washout mechanism in a central Italian region, *Atmospheric Environment*, 20, 125-128, 1986.
- 685 Ferrara, R., Mazzolai, B., Lanzillotta, E., Nucaro, E., and Pirrone, N.: Volcanoes as emission sources of atmospheric mercury in the Mediterranean basin, *The Science of The Total Environment*, 259, 115-121, 2000.
- Friedli, H., Radke, L., and Lu, J.: Mercury in smoke from biomass fires, *Geophysical Research Letters*, 28, 3223-3226, 2001.
- 690 GDAL - Geospatial Data Abstraction Library: Version 2.1.1, Open Source Geospatial Foundation: <http://gdal.osgeo.org>, 2016.
- Glass, G. E., and Sorensen, J. A.: Six-year trend (1990-1995) of wet mercury deposition in the Upper Midwest, USA, *Environmental Science and Technology*, 33, 3303-3312, 1999.
- Google Earth Engine: A planetary-scale geospatial analysis platform: <https://earthengine.google.com>, 2015.
- 695 Gustin, M. S., Lindberg, S. E., and Weisberg, P. J.: An update on the natural sources and sinks of atmospheric mercury, *Appl Geochem*, 23, 482-493, 2008.
- Helsel, D.: *Statistics for Censored Environmental Data Using Mintab and R*, 2nd Edition ed., Wiley Publishing, 2012.
- Jaeglé, L.: *Atmospheric long-range transport and deposition of mercury to Alaska*, Department of Atmospheric Sciences, University of Washington, Seattle, A report to the Alaska Department of Environmental Conservation, 2010.
- 700 Karagas, M. R., Choi, A. L., Oken, E., Horvat, M., Schoeny, R., Kamai, E., Cowell, W., Grandjean, P., and Korrick, S.: Evidence on the Human Health Effects of Low-Level Methylmercury Exposure, *Environ Health Persp*, 120, 799-806, Doi 10.1289/Ehp.1104494, 2012.
- Laird, B. D., Goncharov, A. B., Egeland, G. M., and Chan, H. M.: Dietary Advice on Inuit Traditional Food Use Needs to Balance Benefits and Risks of Mercury, Selenium, and n3 Fatty Acids, *J. Nutr.*, 143, 923-930, 10.3945/jn.112.173351, 2013.
- 705 Lamborg, C. H., Fitzgerald, W. F., Vandal, G. M., and Rolffhus, K. R.: Atmospheric mercury in Northern Wisconsin : sources and species, *Water Air and Soil Pollution*, 80, 189-198, 1995.

- Landis, M. S., Vette, A. F., and Keeler, G. J.: Atmospheric Mercury in the Lake Michigan Basin: Influence of the Chicago/Gary Urban Area, *Environ Sci Technol*, 36, 4508-4517, 10.1021/es011216j, 2002.
- 710 Lawson, N. M., and Mason, R. P.: Accumulation of mercury in estuarine food chains, *Biogeochemistry*, 40, 235-247, Doi 10.1023/A:1005959211768, 1998.
- Lee, K., Hur, S. D., Hou, S., Hong, S., Qin, X., Ren, J., Liu, Y., Rosman, K. J. R., Barbante, C., and Boutron, C. F.: Atmospheric pollution for trace elements in the remote high-altitude atmosphere in central Asia as recorded in snow from Mt. Qomolangma (Everest) of the Himalayas, *Sci Total Environ*, 404, 171-181, <http://dx.doi.org/10.1016/j.scitotenv.2008.06.022>, 2008.
- 715 NADA: Nondetects And Data Analysis for environmental data. R package version 1.5-6.: <http://CRAN.R-project.org/package=NADA>, access: January 2015, 2013.
- Leitch, D. R., Carrie, J., Lean, D., Macdonald, R. W., Stern, G. A., and Wang, F. Y.: The delivery of mercury to the Beaufort Sea of the Arctic Ocean by the Mackenzie River, *Sci Total Environ*, 373, 178-195, DOI 10.1016/j.scitotenv.2006.10.041, 2007.
- 720 Lindberg, S. E., Brooks, S., Lin, C.-J., Scott, K. J., Landis, M. S., Stevens, R. K., Goodsite, M., and Richter, A.: Dynamic Oxidation of Gaseous Mercury in the Arctic Troposphere at Polar Sunrise, *Environmental Science and Technology*, 36, 1245-1256, 2002.
- Loseto, L. L., Stern, G. A., and Ferguson, S. H.: Size and biomagnification: How habitat selection explains beluga mercury levels, *Environ Sci Technol*, 42, 3982-3988, Doi 10.1021/Es7024388, 2008.
- 725 Lyman, S. N., and Gustin, M. S.: Speciation of atmospheric mercury at two sites in northern Nevada, USA, *Atmospheric Environment*, 42, 927-939, 2008.
- Lynam, M. M., Dvonch, J. T., Hall, N. L., Morishita, M., and Barres, J. A.: Spatial patterns in wet and dry deposition of atmospheric mercury and trace elements in central Illinois, USA, *Environmental Science and Pollution Research*, 21, 4032-4043, 2014.
- 730 Macdonald, R. W., and Bowers, J. M.: Contaminants in the arctic marine environment: Priorities for protection, *ICES J. Mar. Sci.*, 53, 537-563, 10.1006/jmsc.1996.0077, 1996.
- Mason, R. P., Lawson, N. M., and Sullivan, K. A.: The concentration, speciation and sources of mercury in Chesapeake Bay precipitation, *Atmospheric Environment*, 31, 3541-3550, 1997.
- 735 Mather, T. A., and Pyle, D. M.: Volcanic emissions of mercury to the atmosphere: global and regional inventories. Comment, *Sci Total Environ*, 327, 323-329, DOI 10.1016/j.scitotenv.2003.08.031, 2004.
- Mitchell, C. P. J., Kolka, R. K., and Fraver, S.: Singular and Combined Effects of Blowdown, Salvage Logging, and Wildfire on Forest Floor and Soil Mercury Pools, *Environ Sci Technol*, 46, 7963-7970, Doi 10.1021/Es300133h, 2012.
- National Atmospheric Deposition Program (NADP): about the NADP concentration and deposition maps: <http://nadp.sws.uiuc.edu/data/mapProcess.aspx>, access: 08/24.2016, 2016.
- 740 Nriagu, J., and Becker, C.: Volcanic emissions of mercury to the atmosphere: global and regional inventories, *Sci Total Environ*, 304, 3-12, 2003.
- Obrist, D., Moosmueller, H., Schuermann, R., Chen, L. W. A., and Kreidenweis, S. M.: Particulate-phase and gaseous elemental mercury emissions during biomass combustion: Controlling factors and correlation with particulate matter emissions, *Environ Sci Technol*, 42, 721-727, 10.1021/es071279n, 2008.
- 745 Outridge, P. M., Macdonald, R. W., Wang, F., Stern, G. A., and Dastoor, A. P.: A mass balance inventory of mercury in the Arctic Ocean, *Environmental Chemistry*, 5, 89-111, 2008.
- Pacyna, J. M., Travnikov, O., Simone, F. d., Hedgecock, I. M., Sundseth, K., Pacyna, E. G., Steenhuisen, F., Pirrone, N., Munthe, J., and Kindbom, K.: Current and future levels of mercury atmospheric pollution on a global scale, 2016.
- 750 Pirrone, N., and Mason, R.: Mercury fate and transport in the global atmosphere, Dordrecht, The Netherlands: Springer. DOI, 10, 978-970, 2009.
- Poissant, L., and Pilote, M.: Mercury concentrations in single event precipitation in southern Quebec, *The Science of The Total Environment*, 213, 65-72, 1998.

- Pyle, D. M., and Mather, T. A.: The importance of volcanic emissions for the global atmospheric mercury cycle, *Atmospheric Environment*, 37, 5115-5124, 2003.
- 755 Python Language Reference, version 2.7: <http://www.python.org>.
- R: a language and environment for statistical computing.: <http://www.R-project.org/>, 2014.
- Rasmussen, R., Baker, B., Kochendorfer, J., Meyers, T., Landolt, S., Fischer, A. P., Black, J., Theriault, J. M., Kucera, P., Gochis, D., Smith, C., Nitu, R., Hall, M., Ikeda, K., and Gutmann, E.: HOW WELL ARE WE MEASURING SNOW? The NOAA/FAA/NCAR Winter Precipitation Test Bed, *B Am Meteorol Soc*, 93, 811-829, 10.1175/Bams-D-11-00052.1, 2012.
- 760 Reimann, C., Filzmoser, P., Garrett, R. G., and Dutter, R.: Statistical data analysis explained: applied environmental statistics with R, (Sirsi) i9780470985816, Wiley Online Library, 2008.
- psych: Procedures for Personality and Psychological Research: <http://CRAN.R-project.org/package=psych>, 2014.
- NCEP Climate Forecast System Version 2 (CFSv2) 6-hourly Products. Research Data Archive at the National Center for Atmospheric Research, Computational and Information Systems Laboratory: <http://dx.doi.org/10.5065/D61C1TXF>, access: 08/15/2016, 2011.
- 765 Savina, M., Schächli, B., Molnar, P., Burlando, P., and Sevruk, B.: Comparison of a tipping-bucket and electronic weighing precipitation gage for snowfall, *Atmospheric Research*, 103, 45-51, <http://dx.doi.org/10.1016/j.atmosres.2011.06.010>, 2012.
- 770 Selin, N. E., and Jacob, D. J.: Seasonal and spatial patterns of mercury wet deposition in the United States: Constraints on the contribution from North American anthropogenic sources, *Atmospheric Environment*, 42, 5193-5204, 10.1016/j.atmosenv.2008.02.069, 2008.
- Sheu, G. R.: Update on the APMMN and Progress on Wet Deposition Sample Analysis, 2017.
- Steffen, A., Douglas, T., Amyot, M., Ariya, P., Aspö, K., Berg, T., Bottenheim, J., Brooks, S., Cobbett, F., Dastoor, A., Dommergue, A., Ebinghaus, R., Ferrari, C., Gardfeldt, K., Goodsite, M. E., Lean, D., Poulain, A. J., Scherz, C., Skov, H., Sommar, J., and Temme, C.: A synthesis of atmospheric mercury depletion event chemistry in the atmosphere and snow, *Atmospheric Chemistry and Physics*, 8, 1445-1482, 2008.
- 775 Stow, J., Krümmel, E., Leech, T., and Donaldson, S.: What is the Impact of Mercury Contamination on Human Health in the Arctic?, *Arctic Monitoring and Assessment Programme*, Oslo, pp. 159-170, 2011.
- 780 Streets, D. G., Devane, M. K., Lu, Z. F., Bond, T. C., Sunderland, E. M., and Jacob, D. J.: All-Time Releases of Mercury to the Atmosphere from Human Activities, *Environ Sci Technol*, 45, 10485-10491, 10.1021/Es202765m, 2011.
- Tan, S. W., Meiller, J. C., and Mahaffey, K. R.: The endocrine effects of mercury in humans and wildlife, *Crit Rev Toxicol*, 39, 228-269, Pii 909432267
- 785 Doi 10.1080/10408440802233259, 2009.
- Tchounwou, P. B., Yedjou, C. G., Patolla, A. K., and Sutton, D. J.: Heavy metal toxicity and the environment, in: *Molecular, clinical and environmental toxicology*, Springer, 133-164, 2012.
- Turetsky, M. R., Harden, J. W., Friedli, H. R., Flannigan, M., Payne, N., Crock, J., and Radke, L.: Wildfires threaten mercury stocks in northern soils, *Geophys. Res. Lett.*, 33, 6 pp. 10.1029/2005GL025595, 2006.
- 790 Veyseyre, A., Moutard, K., Ferrari, C., Van de Velde, K., Barbante, C., Cozzi, G., Capodaglio, G., and Boutron, C.: Heavy metals in fresh snow collected at different altitudes in the Chamonix and Maurienne valleys, French Alps: initial results, *Atmospheric Environment*, 35, 415-425, 10.1016/s1352-2310(00)00125-4, 2001.
- Walker, J. B., Houseman, J., Seddon, L., McMullen, E., Tofflemire, K., Mills, C., Corriveau, A., Weber, J. P., LeBlanc, A., Walker, M., Donaldson, S. G., and Van Oostdam, J.: Maternal and umbilical cord blood levels of mercury, lead, cadmium, and essential trace elements in Arctic Canada, *Environ Res*, 100, 295-318, DOI 10.1016/j.envres.2005.05.006, 2006.
- 795 Watras, C. J., and Bloom, N. S.: Mercury and Methylmercury in Individual Zooplankton - Implications for Bioaccumulation, *Limnol Oceanogr*, 37, 1313-1318, 1992.

800 Webster, J. P., Kane, T. J., Obrist, D., Ryan, J. N., and Aiken, G. R.: Estimating mercury emissions resultign from wildfires in forests of the Western United States, *Sci Total Environ*, <http://dx.doi.org/10.1016/j.scitotenv.2016.01.166>, 2016.

Wedepohl, K. H.: The Composition of the Continental-Crust, *Geochim. Cosmochim. Acta*, 59, 1217-1232, 1995.

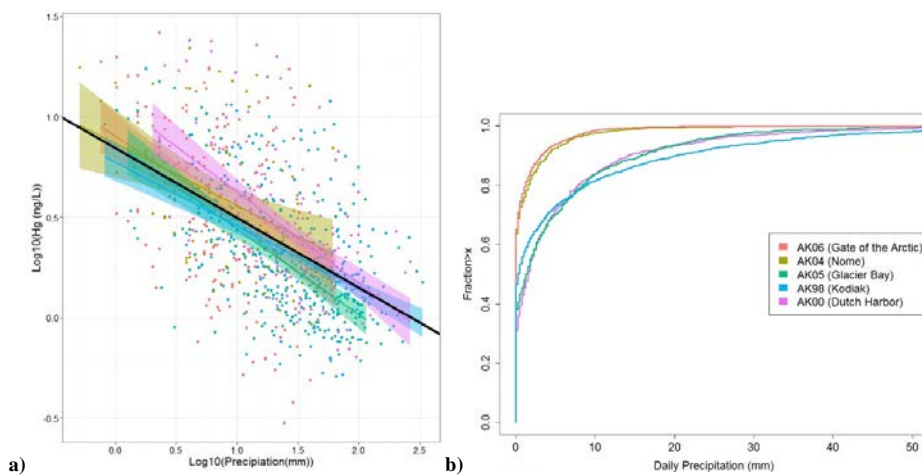
White, E. M., Keeler, G. J., and Landis, M. S.: Spatial variability of mercury wet deposition in eastern Ohio: summertime meteorological case study analysis of local source influences, *Environ Sci Technol*, 43, 4946-4953, 2009.

805 Wickham, H.: *ggplot2: elegant graphic for data analysis*, Springer Verlag, New York, USA, 2009.

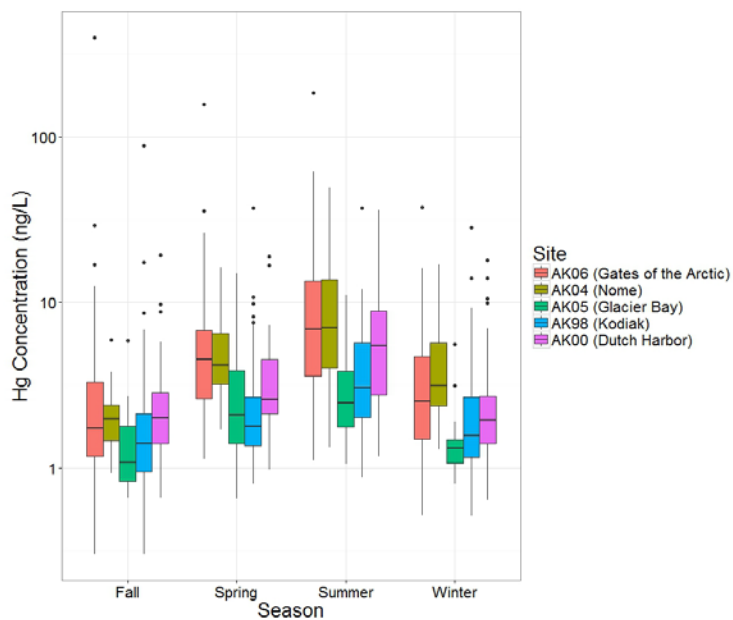
Wiedinmyer, C., Quayle, B., Geron, C., Belote, A., McKenzie, D., Zhang, X., O'Neill, S., and Wynne, K.: Estimating emissions from fires in North America for air quality modeling, *Atmospheric Environment*, 40, 3419-3432, 2006.

Wong, C. S., Duzgoren-Aydin, N. S., Aydin, A., and Wong, M. H.: Sources and trends of environmental mercury emissions in Asia, *Sci Total Environ*, 368, 649-662, 2006.

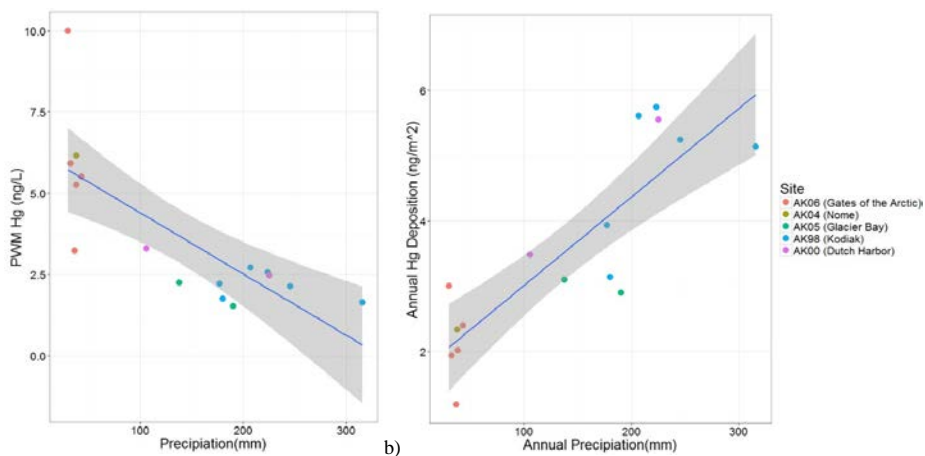
810 Yang, D., Kane, D. L., Hinzman, L. D., Goodison, B. E., Metcalfe, J. R., Louie, P. Y. T., Leavesley, G. H., Emerson, D. G., and Hanson, C. L.: An evaluation of the Wyoming Gauge System for snowfall measurement, *Water Resources Research*, 36, 2665-2677, 10.1029/2000WR900158, 2000.



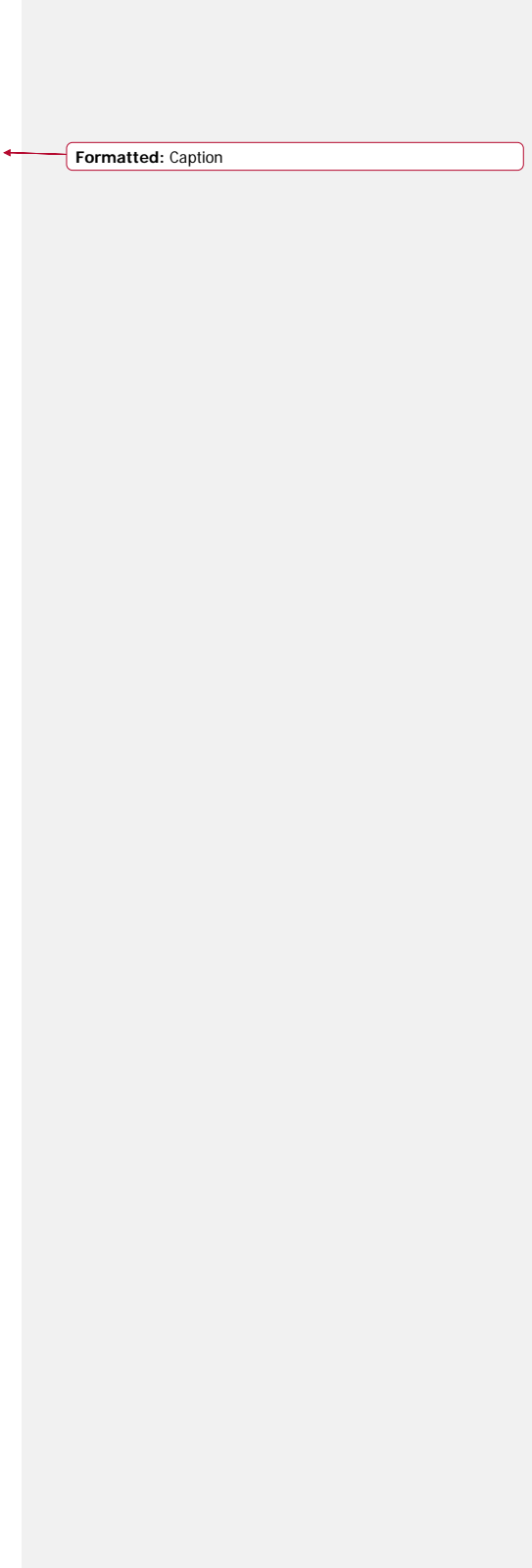
815 **Figure 1. a) Scatterplots of observed Hg concentrations and precipitation amounts, separated by station. The black line shows the overall regression using all sites/all data. A clear dilution effect is observed at all sites. b) Empirical cumulative distribution plot of daily precipitation at five monitoring stations in Alaska (plot has been cropped at 50 mm). Distinct differences in storm size are observed between the northern (red and gold lines) and southern stations (green, blue, and purple lines).**



820
 Figure 2. Summary boxplot of Hg concentrations separated by monitoring station and collection season. Similar seasonal trends are observed at each site with the highest concentrations occurring in summer and lowest concentrations in fall. [Spring \(March, April, May\)](#), [Summer \(June, July, August\)](#), [Fall \(September, October, November\)](#), [Winter \(December, January, February\)](#).



825
 a) Plot of annual precipitation-weighted mean (PWM) Hg concentration versus annual precipitation (mm). Linear regression analysis shows a significant relationship with a correlation coefficient $R^2=0.557$, $p\text{-value} < 0.001$. b) Plot of annual Hg deposition versus annual precipitation (mm). Linear regression analysis shows a significant relationship with a correlation coefficient of $R^2=0.7141$, $p\text{-value} < 0.001$.



Formatted: Caption

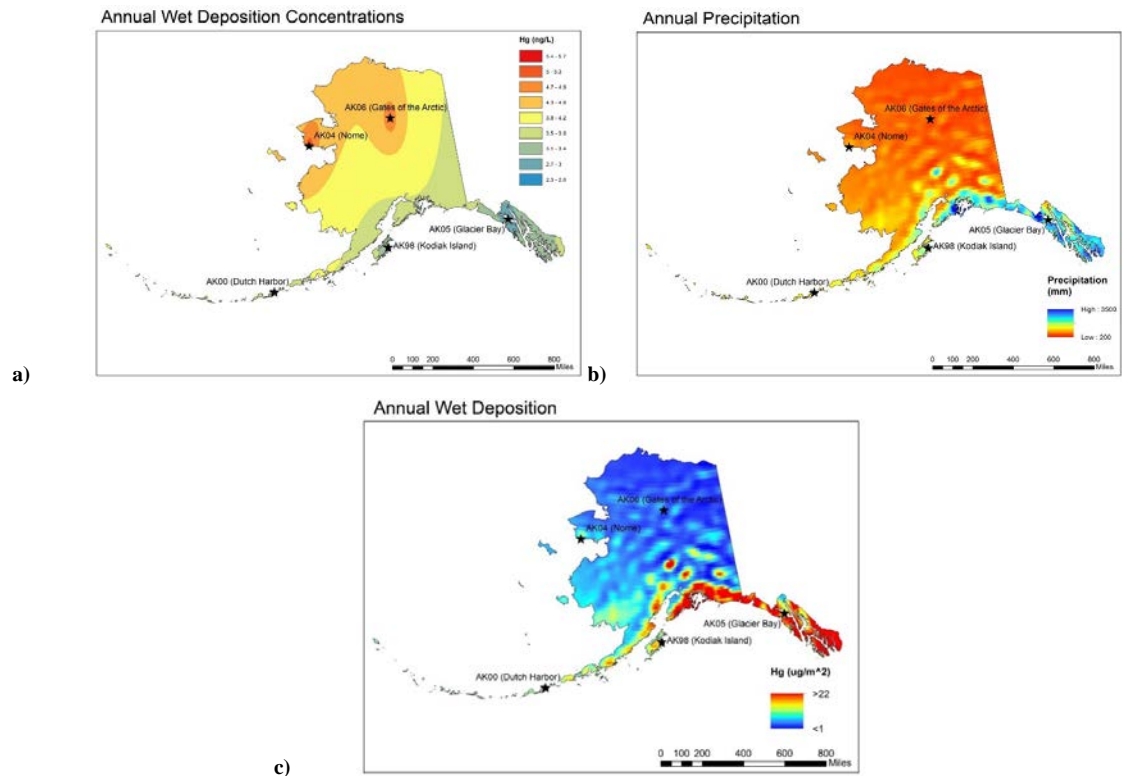
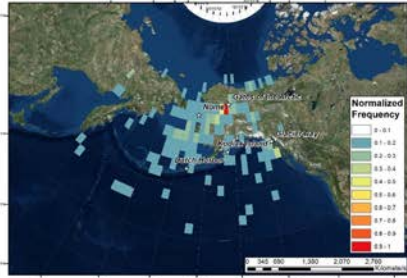


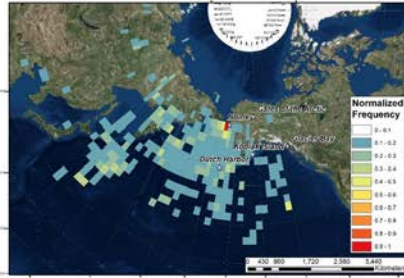
Figure 4. Average Annual Hg deposition maps for the state of Alaska: a) Inverse distance weighted concentration layer; b) NCEP Climate Forecast System Precipitation 2007-2015 annual average; c) Hg deposition estimates. Maps show large-scale concentration gradients (north/south) largely due to precipitation differences with total loading being highly dependent on precipitation.

835

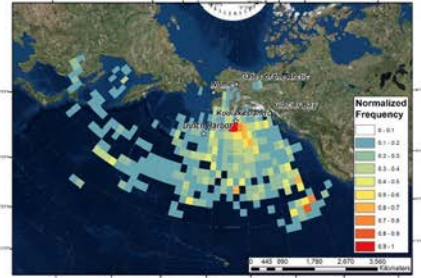
AK06 (Gates of the Arctic)
2014 Precipitation Weighted Normalized Frequency



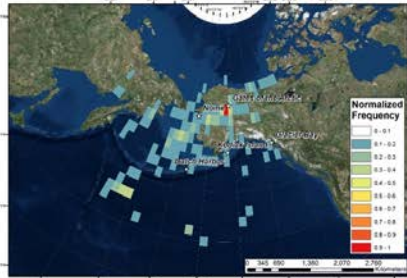
AK04 (Nome)
2014 Precipitation Weighted Normalized Frequency



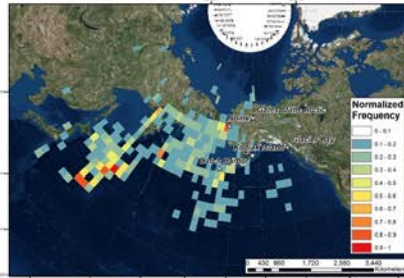
AK98 (Kodiak Island)
2014 Precipitation Weighted Normalized Frequency



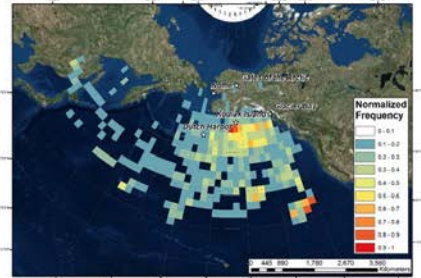
AK06 (Gates of the Arctic)
2014 Deposition Weighted Normalized Frequency

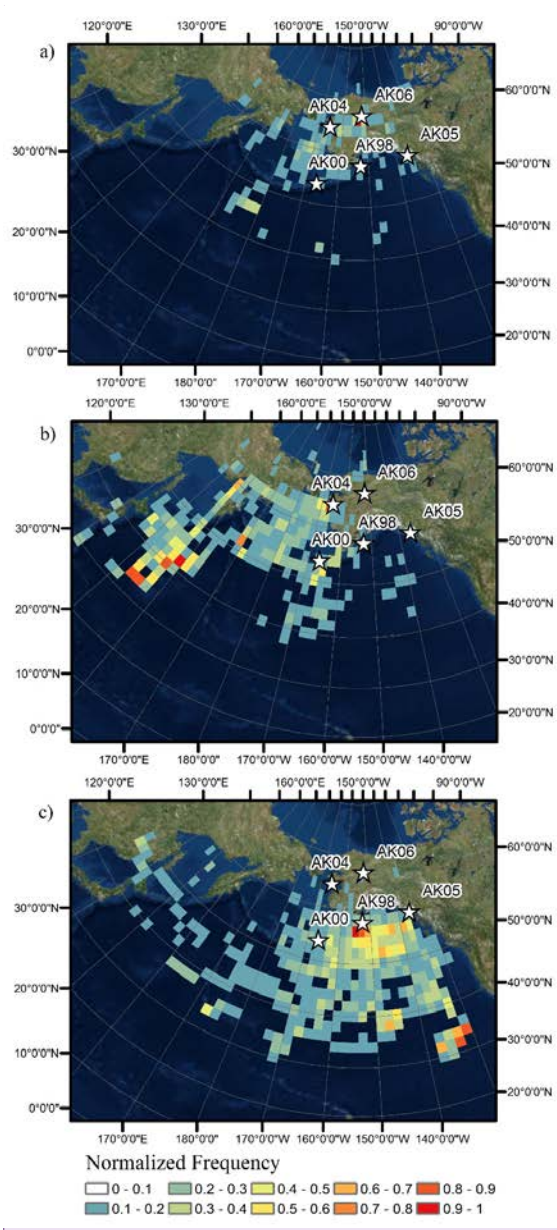


AK04 (Nome)
2014 Deposition Weighted Normalized Frequency



AK98 (Kodiak Island)
2014 Deposition Weighted Normalized Frequency



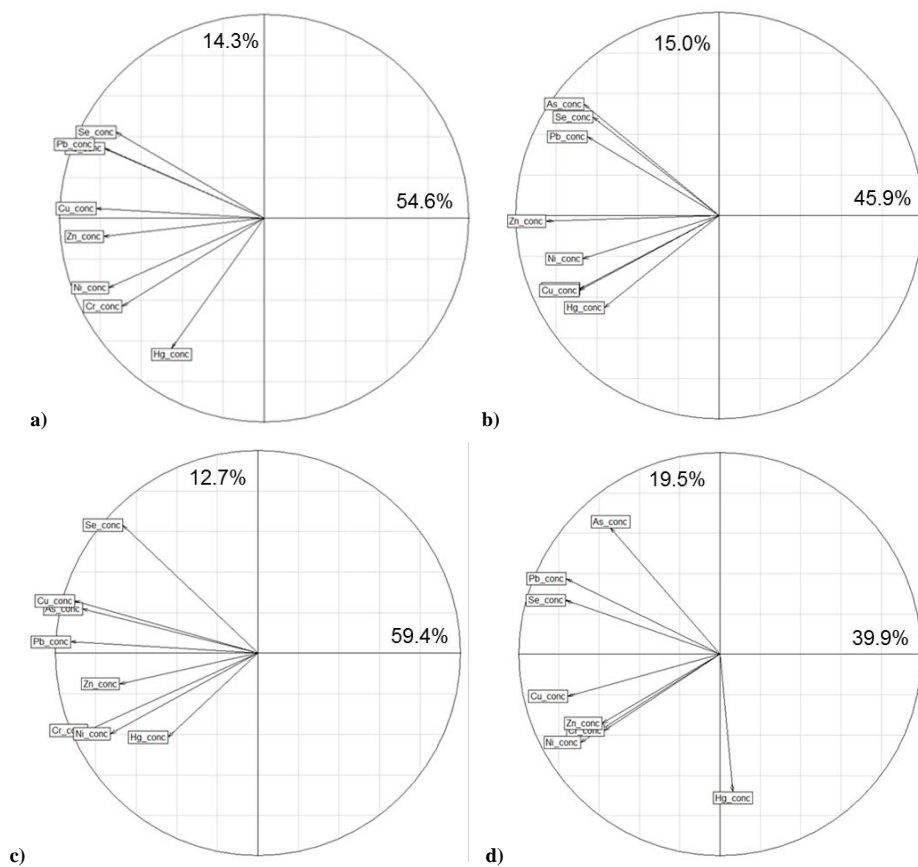


840 Figure 5. Normalized-frequency maps weighted by Hg deposition for top) Gates of the Arctic (AK06), middle) Nome (AK04), and bottom) Kodiak Island (AK98).

Commented [OD14]: Please remove the precipitation maps, I think reviewer 2 is correct.

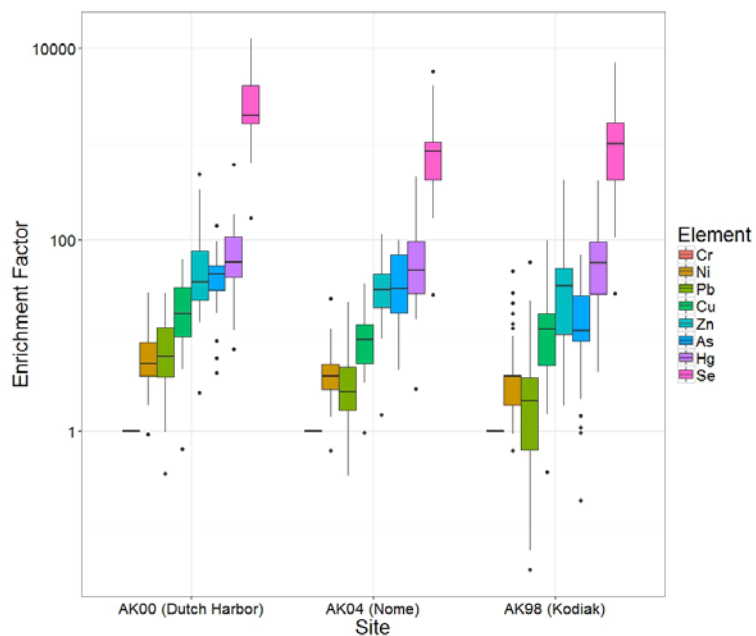
|

Formatted: Caption



845

Figure 6. Trace metal rank-based principal component analysis bipolots of component 1 (x-axis) versus component 2 (y-axis) for a) All Sites, b) Dutch Harbor, c) Nome, and d) Kodiak Island. Values represent the % variance explained by each relative component.



850

Figure 7. Summary boxplot of enrichment factors separated by site. Enrichment factors are calculated using Chromium as the conservative tracer.

Table 1. Overview of available data coverage for each station.

Station ID	AK06	AK04	AK05	AK98	AK00
Station Name	Gates of the Arctic National Park	Nome	Glacier Bay National Park	Kodiak	Dutch Harbor
Latitude	66.906	64.506	58.457	57.719	53.845
Longitude	-151.683	-165.396	-135.867	-152.562	-166.505
Elevation (m)	630	15	2	7	58
Start Measurements	11/11/2008	09/25/2013	03/16/2010	09/18/2007	09/26/2009
Stop Measurements	10/27/2015	09/29/2015	05/21/2013	09/29/2015	09/30/2015
# of Weeks	362	103	165	418	312
# of Hg Concentrations (QR A and B)	216	67	137	321	145
# of Hg Depositions (QR A and B)	267	85	144	351	152
Data Coverage (Deposition)	74%	83%	87%	84%	49%

855

Table 2. Summary statistics of Hg concentrations observed at the five deposition stations, and ANOVA analysis and post-hoc comparisons to test for statistical differences in Hg concentrations among different stations. ANOVA analyses were performed after removal of outliers (concentrations > 26.14 ng L⁻¹).

Station ID	AK06	AK04	AK05	AK98	AK00
Station Name	Gates of the Arctic National Park	Nome	Glacier Bay National Park	Kodiak	Dutch Harbor
Hg concentrations (ng L⁻¹)					
# Outliers Removed (>26.14 ng L ⁻¹)	11	1	0	4	1
Mean	5.3	5.5	2.6	2.7	4.0
Median	3.6	3.5	1.8	1.8	2.3
Standard Deviation	4.9	5.0	2.5	2.4	4.4
Minimum	0.3	0.9	0.7	0.3	0.6
Maximum	26.1	22.0	15.0	17.4	24.0
ANOVA Results [Log10(Hg(ng L⁻¹))*Season*Site]					
	Df	SS	RSS	AIC	F-value
Season	3	90.91	502.35	-440.70	62.46
Site	4	57.06	468.51	-503.25	29.40
Season: Site Interaction	12	8.60	420.04	-614.03	1.48
Post-Hoc Comparisons					
Season					
	Diff	Lower	Upper	P-value	
Spring-Fall	0.4722	0.3016	0.6429	<0.001	
Summer-Fall	0.9155	0.7492	1.0818	<0.001	
Winter-Fall	0.1919	0.0174	0.3664	0.0245	
Summer-Spring	0.4433	0.2725	0.6141	<0.001	
Winter-Spring	-0.2803	-0.4591	-0.1015	<0.001	
Winter-Summer	-0.7236	-0.8983	-0.5489	<0.001	
Site					
	Diff	Lower	Upper	P-value	
Dutch Harbor-Nome	0.2498	-0.0333	0.5328	0.1129	
Dutch Harbor-Kodiak	-0.3614	-0.5528	-0.1701	<0.001	
Dutch Harbor-Glacier Bay	-0.4630	-0.6903	-0.2358	<0.001	
Dutch Harbor-Gates of the Arctic	0.1261	-0.0812	0.3333	0.4577	
Nome-Kodiak	-0.6112	-0.8689	-0.3536	<0.001	
Nome-Glacier Bay	-0.7128	-0.9981	-0.4275	<0.001	
Nome-Gates of the Arctic	-0.1237	-0.3934	0.1459	0.7193	
Kodiak-Glacier Bay	-0.1016	-0.2963	0.0931	0.6106	
Kodiak-Gates of the Arctic	0.4875	0.3166	0.6584	<0.001	
Glacier Bay-Gates of the Arctic	0.5891	0.3788	0.7994	<0.001	

Table 3. Summary statistics of NADP MDN annual estimates of precipitation-weighted mean concentration, deposition, and precipitation for five monitoring sites in Alaska.

Station ID	AK06	AK04	AK05	AK98	AK00
Station Name	Gates of the Arctic National Park	Nome	Glacier Bay National Park	Kodiak	Dutch Harbor
# of Years	5	1	2	6	2
Hg PWM concentrations (ng L⁻¹)					
Mean	5.980	6.153	1.887	2.167	2.875
Standard Deviation	2.474		0.515	0.431	0.581
Median	5.509	6.153	1.887	2.177	2.875
Minimum	3.224	6.153	1.523	1.628	2.464
Maximum	9.997	6.153	2.251	2.709	3.286
Hg deposition (ng m⁻²)					
Mean	2.108	2.338	3.002	4.801	4.518
Standard Deviation	0.665	NA	0.145	1.035	1.466
Median	2.018	2.338	3.002	5.191	4.518
Minimum	1.188	2.338	2.899	3.137	3.481
Maximum	3.004	2.338	3.104	5.743	5.554
Precipitation (mm)					
Mean	363.1	380.0	1641.7	2249.4	1657.4
Standard Deviation	52.1	0.0	370.6	515.3	845.2
Median	368.6	380.0	1641.7	2153.2	1657.4
Minimum	300.5	380.0	1379.6	1773.3	1059.7
Maximum	435.1	380.0	1903.8	3157.9	2255.1

865

Table 4. Trace metal summary statistics using both Maximum Likelihood Estimation and ½ MDL substitution techniques.

Maximum Likelihood Summary Statistics (ug L⁻¹; n=131)				
	n < MDL	median	mean	std deviation
Arsenic	47	0.0216	0.1936	1.7240
Chromium	45	0.0222	0.0793	0.2719
Copper	1	0.1370	0.2525	0.3907
Lead	7	0.0389	0.1080	0.2799
Nickel	57	0.0360	0.2782	2.1331
Selenium	31	0.0635	0.1125	0.1646
Zinc	2	1.4033	2.9077	5.2769